Design and Development of Hydrophobic and Protective Polymer-based Spray Coatings for Treating Glass Surfaces in Building and Automotive Applications

by

Wing Yi Pao

A thesis submitted to the
School of Graduate and Postdoctoral Studies in partial
fulfillment of the requirements for the degree of

Master of Applied Science

Department of Automotive, Mechanical and Manufacturing Engineering

Faculty of Engineering and Applied Science

Ontario Tech University

Oshawa, Ontario, Canada

August 2019

THESIS EXAMINATION INFORMATION

Submitted by: **Wing Yi Pao**

Master of Applied Science in **Automotive Engineering**

Thesis title: Design and Development of Hydrophobic and Protective Polymer-based Spray Coatings for Treating Glass Surfaces in Building and Automotive Applications

An oral defense of this thesis took place on August 21, 2019 in front of the following examining committee:

Examining Committee:

Chair of Examining Committee	Dr. Dipal Patel
Research Supervisor	Dr. Remon Pop-Iliev
Research Co-supervisor	Dr. Ghaus Rizvi
Examining Committee Member	Dr. Xianke Lin
Thesis Examiner	Dr. Amirkianoosh Kiani, UOIT

The above committee determined that the thesis is acceptable in form and content and that a satisfactory knowledge of the field covered by the thesis was demonstrated by the candidate during an oral examination. A signed copy of the Certificate of Approval is available from the School of Graduate and Postdoctoral Studies.

ABSTRACT

Glass surfaces in buildings and vehicles are susceptible to two common problems: unrestricted energy transmittance of light-waves resulting in increased HVAC costs, and reduced visibility as a consequence of wetting during precipitation; which is an accident hazard for automobiles. In this context, the surface properties of the glass can be altered and enhanced by deliberately applying hydrophobic and/or protective topical coatings. This research focuses on evaluating the performances of multiple newly-formulated low-cost spray coatings based on polymethylmethacrylate (PMMA) and its blends with various polymers. The experimental comparative characterization study included: transmittance measurement, microstructure visualization, and wettability quantification under static and dynamic conditions. The obtained results indicated that PMMA enhanced the transparency and adhesion to the glass, whereas the addition of secondary polymers reduced wetting and increased blockage of ultraviolet and infrared light-waves. The developed coatings proved their implementation potential for applications where thermal radiation shielding and water repellency are required.

Keywords: Spray coating; Polymer blends; Transmittance; Water contact angle; Dynamic droplet behavior

AUTHOR'S DECLARATION

I hereby declare that this thesis consists of original work of which I have authored. This is a true copy of the thesis, including any required final revisions, as accepted by my examiners.

I authorize the Ontario Tech University to lend this thesis to other institutions or individuals for the purpose of scholarly research. I further authorize Ontario Tech University to reproduce this thesis by photocopying or by other means, in total or in part, at the request of other institutions or individuals for the purpose of scholarly research. I understand that my thesis will be made electronically available to the public.

Roxana

Wing Yi (Roxana) Pao

STATEMENT OF CONTRIBUTIONS

Part of the work described in Chapter 4 has been published in the Proceedings of the 2019 Canadian Society for Mechanical Engineering (CSME) International Congress as:

Pao, W.Y., Pop-Iliev, R., Rizvi, G., "Investigative Experimental Study of the Wetting Behavior of Transparent Coatings of PMMA Blends with PVC/PS/PVDF/PDMS", Proceedings of CSME-CFDSC Congress 2019, 2019.

ACKNOWLEDGEMENTS

First of all I would like to thank my parents for their unconditional loving from the other end of the globe, they have been very supportive in both decision making and finance.

Secondly, I would like to thank my supervisors Dr. Remon Pop-Iliev and Dr. Ghaus Rizvi for their guidance and providing me the facility to explore in the polymer-based fabrication field, as well as their encouragements on publications and conference opportunities.

Thirdly, I would like to thank the Nathan and Marvin Goldman Durham Homes Graduate Award for the financial support in the school year of 2017 – 2018 and their approval on the visions of sustainability by reducing the use of energy through indoor climatic control.

Next I would like to thank you our lab post-doctoral fellow Carlos, and lab-mates Pedram, Utkarsh, Isha, Nabeel, Tariq, Ashique for all the helps and discussions on equipment set-ups and the data analyses they have been providing.

Lastly, I would like to thank the NSERC's Chairs in Design Engineering Program and the NSERC's Discovery Development Grant for the financial support for this research.

TABLE OF CONTENTS

LIST OF TABLES

CHAPTER 3

CHAPTER 4

LIST OF FIGURES

CHAPTER 2

CHAPTER 3

CHAPTER 4

LIST OF ABBREVIATIONS AND SYMBOLS

NHTSA	National Highway Traffic Safety Administration
PMMA	Poly (methyl methacrylate)
PVC	Poly (vinyl chloride)
PS	Poly (styrene)
PVDF	Poly (vinylidene difluoride)
PDMS	Poly (dimethyl siloxane)
DMCPS	Decamethylcyclopentasiloxane
Tg	Glass transition temperature
H-	Hydrogen bonding
VOC	Volatile organic compounds
HAP	Hazardous air pollutants
δ	Solubility parameter
δs	Hildebrand solvent solubility parameter
δp	Hildebrand polymer solubility parameter
δd	Hansen dispersion solubility parameter
δp	Hansen polar solubility parameter
δh	Hansen hydrogen bond solubility parameter
R	Radius threshold of solute
WLF	Williams-Landel-Ferry equation
C_1, C_2	Empirical constants for WLF equation
η	Viscosity
A_t	Shift factor
τ	Relaxation time
T, T_o	Temperature and reference temperature
^oC	Degree Celsius
W/mK	Watts per meter-Kevin
UV	Ultraviolet
IR	Infrared
VL	Visible light

WCA	Water contact angle
deg, ^{o}	Degree
DMF	Dimethylformamide
THF	Tetrahydrofuran
NH_4HCO_3	Ammonium bicarbonate
wt%	Concentration in weight percent
FTIR	Fourier-Transform Infrared
f1, f2	Volume fractions for solid and air
θ1, θ2	Contact angle with solid and air
γ	Interfacial energy
L	Liquid
S	Solid
V	Vapor
θW	Wenzel contact angle
θY	Young's contact angle
ms	Millisecond
μL	Microliter
nm	Nanometer
mm	Millimeter
SHGC, g	Solar heat gain coefficient
T	Transmittance
A	Absorbed energy
Q	Energy gain
A	Area
G	Irradiance
W/m^2K	Watts per meter square Kevin
ABS	Acrylonitrile butadiene
PC	Poly (carbonate)
Mw	Molecular weight
g/mol	Grams per mole
mN/m	milli-Newton per meter

$MPa^{1/2}$	Square root of megapascal
“	Inch
TGA	Thermogravimetric analysis
%/min	Percent per minute
RPM	Revolution per minute
g	Gram
mL	Milliliter
psi	Pounds per square inch
rej	Rejection
w/	With
w/o	Without
km/hr	Kilometer per hour
d	Diameter of water droplet
V	Velocity
exp	Experimental
S.D.	Standard deviations

Chapter 1. Introduction

1.1 Motivation and Statement of the Problem

Visibility is an important criterion for the safety of moving vehicles. Low visibility due to adhesion of water droplets on windshields and windows can severely impair driver's capability to exert good judgement and coordination. The rising trend of driver-assist systems of sensors and cameras also promotes the need of visibility to remain functional at all times. Reports based on National Highway Traffic Safety Administration (NHTSA) data (Hamilton, B.A.) have indicated that rain is rated to be the most hazardous driving condition when compared to other weather-related events such as snow and fog. Rain combined with dirt and oil can severely impair visibility causing accidents. From the ten-year average statistics (Hamilton, B. A., 2018), there are over 1.2 million accidents annually that are weather-related in the United States, and they accounted for 21% of the total number of accidents. The average number of accidents due to rain is about 0.55 million, contributing to almost 50% of the weather-related crashes.

On the other hand, sunlight is one of the most abundant energy sources. However, most of the solar energy is not being fully utilized by current technologies and is dissipated in the form of heat. This can often be undesirable for homes, office buildings, and automobiles; ironically energy is required to remove the heat. It has been observed that air-conditioning can contribute up to 30% of electricity consumption. Parked vehicles under sunlight can also reach up to 50 ^{o}C within an hour and cause fatality to children and pets. (Garethiya, S., et al., 2015) Whereas in the cold days, heat loss from unprotected glass

windows can be significant and heating of dwellings accounts for approximately 30% of energy usage (Mempouo, B. et al, 2010).

There are a few products available in the market that aim to provide solutions to reject solar transmittance and improve water repellency. However, most of them only address one issue at a time or have only been tested for one particular function. **This research aims to address both issues via a single solution by using a surface coated product, and thus help reduce the environmental impact caused by air conditioning and heating; as well as improve driving safety.**

1.2 Current Trends and Technologies

To control indoor climate passively, conventional methods alter the window transmittance through decreasing the passage of visible light with the use of dark tints. Although this method provides good privacy, it draws concern for visibility at night. 3M is a North America based scientific company that produces primarily tapes and films. 3M's residential window films claims to be able to reflect 78% of solar heat from outdoor in hot days and maintain heat from indoor in cold days.

To obtain a non-wetting surface, NeverWet is a leading hydrophobic coating brand owned by Rust-Oleum, a North America based paint and coating company, it has developed a fabric-friendly 2-step multi-surface spray that prevents sprayed objects from getting wet or dirty. It claims to be superhydrophobic, anti-icing, anti-corrosion, and oleophobic, which are all extremely attractive properties for commercial products,

representing durability and reliability. However, NeverWet's spray is not suggested for glass application as the finished surface is not fully transparent. For vehicle specific applications, Ceramic Pro is one of the global leaders for car body and glass coating that utilizes nano-technology, the coating consists of nano-scale ceramic particles that are dispersed in a polymer solution. The coating has been proven to be an effective paint protection method that lasts between two to three years. Their glass specific product RAIN claims to be hydrophobic with water contact angle of 110^{o} and the hydrophobicity will last up to one year.

Soft99 is a Japan based company that produces automotive wax and coating products. Soff99's Glaco is a transparent and slippery product for glasses that is applied through rubbing with a sponge. Coated windshield surfaces treated with Glaco have shown to attain a hydrophobic state with a water contact angle of 105 ^{o} and sliding angle of 35^{o} (Kato, M., et al., 2011). Soft99 claims that Glaco water droplets can slide away easily without the need of wipers at driving speed of approximately 45 km/hr. However, Kato, M. and others (Kato, M. et al., 2011) found that the performance of Glaco decreased dramatically after abrasion tests with sponge wiping, where contact angle reduces and water droplet does not slide away at the same driving speed, suggesting that the coating can be removed easily. Lastly, RainX glass water repellent is a glass treatment product that contains a transparent ingredient made of a siloxane derivative. The product can be applied to glass through wiping and let dry in air to leave behind a slippery surface, the coating requires re-application within 3 months.

The durable coating products such as Ceramic Pro are expensive due to the use of inorganic particles and the complex surface preparation prior to application; whereas the

inexpensive products such as Glaco and RainX are not durable due to the use of siloxanes which have low adhesion capability. On the other hand, most window films for climatic control are not recommended to be applied on the exterior side of windows to prevent weathering. It is observed that each product targets only a specific function of either water repellency or altering glass transmittance, while both are important desired properties that should be provided to the glass, to improve visibility for safety of road vehicles and reduce the use of energy to improve sustainability.

1.3 Objectives

This research aims to develop an outdoor coating for building windows and vehicle windshields applications, which contains the following combined properties of low cost, water repellent, and resistance to heat gain/loss.

The general objective of this work is to design and develop a variety of coatings and then test, evaluate, and comparatively characterize the suitability of poly(methyl methacrylate) (PMMA) and its blends with various common polymers including poly(vinyl chloride) (PVC), polystyrene (PS), poly(vinylidene difluoride) (PVDF), and poly(dimethyl siloxane) (PDMS) for the targeted applications.

To achieve the general objective, the following specific objectives are carried out:

- To develop appropriate formulated solutions of PMMA and its blends with PVC, PS, PVDF, and PDMS that can be applied as coatings on glass.

- To study the effect of the microstructure and the molecular structure of these coatings on their solar range transmittance and wettability.
- To study the interactions between the coated surfaces and water droplets in both static and dynamic conditions.
- To compare the developed coating with existing products that are available in the market, including 3M outdoor window insulator film, NeverWet spray, and RainX glass water repellent.

1.4 Thesis Outline

Chapter 1 describes the scope of research and justifies the motivation based on the crisis that the energy and transportation sectors face, including increasing environmental impact from the use of air-conditioning and heating, and the increased emphasis of road safety to reduce accident rates. The study aims to provide a proposed solution of incorporating a low-cost polymer-based outdoor coating that can regulate indoor climate and self-clean.

Chapter 2 consists of literature reviews. The background on properties, solubility, and blending of polymers are explained with the focus on materials being used in this research to support the material selection with reference to examples from literature. Models and criteria that contribute to water repellency are presented and were used as reference to characterization planning in Chapter 3 and quantification of results in Chapter 4. The sources of solar heat and heat transfer of windows are reviewed, to demonstrate the solution to reducing the heat gain and loss through electromagnetic waves rejection.

Coating methods are introduced and the advantages of spray deposition technique are stated.

Chapter 3 describes the experimental setup and methodology, including material selections and solution property considerations. The experimental planning and results characterization methods are also presented.

Chapter 4 and 5 present experimental results and conclusions, respectively. The sequence of results presentation is as follow: transmittance, microstructure, static water contact angle, and dynamic water droplet behavior.

1.5 References

Garethiya, S., Himanshu A., Shilpa G., Amit K.E, Gaurav W., and Girishchandra R.Y. "Affordable system for alerting, monitoring and controlling heat stroke inside vehicles." In *2015 International Conference on Industrial Instrumentation and Control (ICIC)*, pp. 1506-1511. IEEE, 2015.

Hamilton, B.A. "Ten-year averages from 2007 to 2016." *Retrieved from Road Weather Management Program-NHTSA: http://www.ops.fhwa.dot.gov/weather/q1_roadimpact. Htm* (2018).

Kato, M., Akinori T., Masahiro S., and Hiromitsu A. "Durable automotive windshield coating and the use thereof." U.S. Patent 8,043,421, issued October 25, 2011.

Mempouo, B., Cooper, E., and Riffat, S.B. "Novel window technologies and the code for sustainable homes in the UK." *International Journal of Low-Carbon Technologies* 5, no. 4 (2010): 167-174.

Chapter 2. Literature Review

2.1 Polymers

2.1.1 Polymer properties

Polymers are generally classified into two main groups as natural and synthetic, natural polymers can be extracted from nature such as proteins, cellulose, and wool; whereas many common polymers including the ones used in this research such as poly(methyl methacrylate) (PMMA), poly(vinyl chloride) (PVC), polystyrene (PS), poly(vinylidene difluoride) (PVDF), and poly(dimethyl siloxane) (PDMS) belong to the synthetic type. Plastics are polymers that consist of chains of repeated units of mono-"mer" which are the building blocks of the long-chain molecular polymeric morphological structures (Callister, W.D., 2000).

The polymer field grew rapidly, since early 20^{th} century when synthetic polymers were first introduced by Leo Baekeland with the invention of Bakelite (Williams, D.J., Neal, R.A., 1971). It opened up opportunities for polymer applications and material development where polymers can be produced with different molecular structures and can be mixed or intrinsically modified with functional groups to achieve desired properties.

Among the synthetic group of polymers, they can be further classified based on the structure. The packing of structures would have an impact on crystallinity and the thermal behavior of polymers. Homopolymers contain only one type of repeating monomer in the linear chains and branches, excessive branching and random ordering would prevent orderly packing and reduce crystallinity. Within the same chain of a homopolymer, the

stereochemical orientation is defined as tacticity. Isotactic arranges the side group on the same side, syndiotactic ones are arranged on alternate sides, and atactic refers to a random order. Copolymers contain two or more types of monomers, the arrangements often depend on the synthesis procedure. The repeating arrangement can be alternate (ABABABAB), block (AAAABBBB), or grated chains onto the main backbone. Figure 2.1 shows the possible oriented structures of homopolymers and copolymers. (Callister, W.D., 2000)

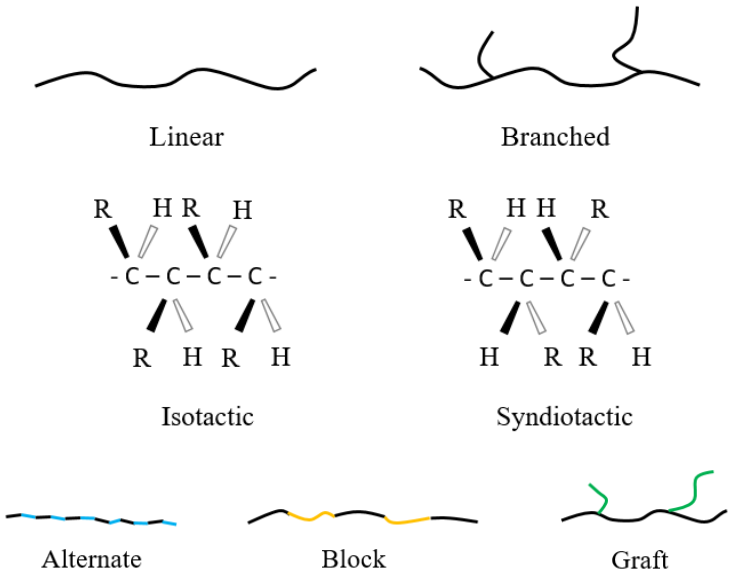

Figure 2.1. Polymer types and orientations.

Polymers are never fully crystalline as it is thermodynamically impossible, polymers are either semi-crystalline or amorphous. The degree of crystallinity directly affects the glass transition temperature (Tg) of a polymer in a reverse relationship. Higher crystallinity tends to lower Tg as crystals are subjected to molecular motion when heated and softens, while amorphous structure tends to be bulkier which inhibits motions and increase Tg. (Schaffer, J.P., et al., 1995)

2.1.2 Polymer solutions

Processing of polymers often involves solidification process from liquid state in order to alter the shape of raw polymer resins, the liquid state can be achieved by melting with heat, or dissolving in appropriate organic solvents. Solvents for organic coatings are usually classified into three categories: weak hydrogen (H-) bonding, hydrogen bond acceptor, and hydrogen bond donor-acceptor. The level of hazard of a solvent is determined by the emission of volatile organic compounds (VOC) and hazardous air pollutants (HAP). Chlorinated solvents are not used in coating industry anymore as it has huge environmental impact that leads to ozone depletion.

Aliphatic and aromatic hydrocarbons are weak H-bonding solvents, aliphatic hydrocarbons are mixtures of chained, branched, and alicyclic hydrocarbons, and they are generally less expensive than aromatic solvents. Aromatic solvents are HAPs but are capable of dissolving a wider range of resins. Esters and ketones are H-bond acceptor solvents, acetone is an example of ketones that is exempt as VOC or HAP. Finally, alcohols and other slow evaporating water-soluble solvents belong to the H-bond acceptor-donor group.

The solubility parameter δ is a standard guide for solvent selections, generally, if both solute and solvent have similar Hildebrand δ values, they are likely to form a dissolved solution, where p and s represent polymer and solvent, respectively in Equation 1. Hansen Solubility parameters δd, δp, δh describe the radius threshold based on 3-dimensional spherical volume of solute as shown in Equation 2, where the subscripts d, p, and h denote dispersion, polar, and hydrogen bond, respectively. The solubility parameter of mixed

solvents can be determined by weighted average using the same formula. (Hansen, C.M., 2002)

$$\left|\delta_s - \delta_p\right| \leq 3.6\ \mathrm{MPa}^{1/2} \qquad (1)$$

$$\left|4\left(\delta_{d2} - \delta_{d1}\right)^2 + \left(\delta_{p2} - \delta_{p1}\right)^2 + \left(\delta_{h2} - \delta_{h1}\right)^2\right|^{1/2} \leq R \qquad (2)$$

Most coatings are formed from solution state, viscosity is a key consideration as the requirements are different for the fabrication methods. During the solvent evaporation process, viscosity of film increases, the solvent molecules will need to diffuse towards the top surface in order to evaporate. Solvent can be retained and baking is one of the most popular methods for complete removal of solvents.

As most binders are amorphous, a solidified layer is determined to have no significant flow being observed under pressure during use of coated parts, and without sticking onto each other if two coated surfaces meet (Jones, F.N., et al., 2007); a crystalline component will therefore aid solidification based on this logic where flow is inhibited. Williams-Landel-Ferry (WLF) equation (Equation 3) determines the required Tg of film such that it does not flow and dry to touch, by incorporating empirical constants of materials C_1 and C_2 (Sanditov, D.S., Razumovskaya, I. V., 2018). The WLF equation can be used to estimate the viscosity η which is essentially related to the shift factor A_t with respect to relaxation time τ (TA Instruments, RN011).

$$\log A_t = \frac{-C_1(T - T_o)}{C_2 + (T - T_o)} \quad ; \quad A_t = \frac{\tau(T)}{\tau(T_g)} = \frac{\eta(T)}{\eta(T_g)} \qquad (3)$$

2.1.3 Poly(methyl methacrylate)

Poly(methyl methacrylate) (PMMA), is well-known for its other names of acrylic and Plexiglas. It is a synthetic thermoplastic and was first discovered by British chemists Hill, R. and Crawford, J. in the 1930s (Ali, U., et al., 2015). PMMA has superior properties over many other polymers, it is highly transparent; excellent resistance to impact, scratch, and weather; and dimensional stable (Zhou, X.D., et al., 2002). PMMA is used in applications such as lenses, vehicle headlight housings, and aircraft windows as it is shatter-proof (Schaffer, J.P., et al., 1995). Additionally, PMMA is recyclable (Charmondusit, K., Seeluangsawat, L., 2009), biocompatible (Petrochenko, P.E., et al., 2017), and biodegradable (Bhat, D.K., Kumar, M.S., 2006).

PMMA has been reported to be able to accommodate different classes of functional materials. **Therefore the current work is not limited to only polymer coatings but can expand the applications in future work to incorporate functional materials as dopants to enhance water repellency and introduce new properties such as conductivity and intelligent response of reversible self-coloring.** For example: Gao, Z. and others (Gao, Z., et al., 2018) have fabricated PMMA composite coating with polyaniline (PANI) to obtain a semi-insulating film for dielectric component application. Soumya, S. and others (Soumya, S., et al., 2016) have reported that PMMA has low thermal conductivity of only 0.2 W/mK but poor for shielding UV and IR, they have attempted to improve the reflectivity of solar irradiation of PMMA by incorporating aluminum doped zinc, a 10^{o}C difference was achieved between wooden box with and without the coating under the test light source. PMMA is also a common choice of material to host organic dyes for light-emitting diode or solar cells applications. Caruso, F. and others (Caruso, F. et al., 2016)

have shown that curing of PMMA can better protect the dye from UV degradation and photo-oxidation.

2.1.4 Poly(vinyl chloride)

PVC is inexpensive and generally targeted for corrosion resistant applications such as on the surface of pipelines. Borisov, B.I. and Markova, G.S. (Borisov, B.I., Markova, G.S., 1975) have studied the changes in PVC coating in underground pipes and found that PVC is prone to aging due to oxidation of air, but it results in increased tensile strength and Tg. Kang, Y. and others (Kang, Y., et al., 2011) have investigated the water and oil behavior on PVC surfaces prepared from dip coating in different ratios of tetrahydrofuran solvent and glacial acetic acid. The PVC coatings prepared without mixed solution was found to be transparent and had water contact angle of about 90^{o}; whereas the ones prepared from acid to solvent volume ratio of 2.5:10 reached the superhydrophobic and superoleophilic state.

2.1.5 Polystyrene

Polystyrene (PS) is another readily available and intensively studied polymer. PS films can be formed relatively easily, and can be found in everyday life such as Styrofoam and clear food containers. PS can also be used as corrosion protection coating, Zhao, Y. and others (Zhao, Y., et al., 2017) have studied the wetting behavior of electrospun PS coating, the coating was deposited on top of porous conductive anti-corrosion PANI/PMMA layer for carbon-steel components. The PS top layer acted as protection to the pores to reduce pathways of corrosion. The sprayed PS had a WCA of 100^{o}, and the PS

coating on top of the Polyaniline/PMMA layer achieved a contact angle that was close to superhydrophobic state due to increased roughness.

2.1.6 Poly(vinylidene difluoride)

PVDF is a semi-crystalline polymer (Aid, S., et al., 2019), it has outstanding weather resistance and is not affected by pollutants, oxidation, and photo-degradation, therefore suitable for outdoor applications (Lopez, G., et al., 2017). Peng, C., and others (Peng, C., et al., 2012) have reported the use of PVDF as anti-icing coating for wind turbine blades. It was believed that reducing the interface between blade surface and water, while increasing the interface between surface and air, can greatly reduce the chance of ice formation. The PVDF coating was dissolved in DMF at 10 wt%, ammonium bicarbonate (NH_4HCO_3) was added in small quantity to aid pore formation to improve roughness. The PVDF coating was measured to have WCA of 102^o, which is an improvement of about 20^o compared to uncoated blade. The PVDF/ NH_4HCO_3 improved the WCA drastically into the superhydrophobic state of 156^o, however the transparency was not discussed.

2.1.7 Poly(dimethyl siloxane)

PDMS belongs to the silicone group of poly-siloxanes, it is a common material being used for water-repellent applications due to its low surface energy. It has other advantages such as transparency and the ability to provide even thickness in coatings. Kronlund, D. and others (Kronlund, D., et al., 2016) have spray coated 10 wt% PDMS dissolved in toluene solvent on granite substrate at different pressures and flow rates, the spray distance was held constant. The measured contact angles of the PDMS coated granite surfaces with

different spraying conditions were all similar, at about 120^{o}, the performance reduced by 10^{o} after 30 freeze-thaw with salt crystallization cycles.

2.1.8 Poly(methyl methacrylate) blends

The solution blends with a two or more solvents and polymers have been found to be effective in achieving a full range of properties at low costs, it can usually lead to improvements on the overall performance. The blended product can potentially be benefited from the combined properties of the separate polymers such as toughness, chemical and flammable resistance, where the use of additives can be eliminated. (Utracki, L.A., Wilkie, C.A., 2002)

The fabrication of semi-crystalline polymers often requires less modifications, as it contains 2-phase structure of both crystalline and amorphous regions, for which the amount of crystallinity can be varied to tailor for desired properties. However amorphous polymers are more brittle and contain only one phase, to fully harvest its properties, it often requires blending to lower the overall Tg for processing, and broaden the range of molecular weights for wider range of applications. (Utracki, L.A., Wilkie, C.A., 2002)

Mixing of solvents on the other hand can alter the solution viscosity, vapor pressure, and surface tensions. For example: Casasda, R. and others (Casasda, R., et al., 2014) have found that increasing the DMF content will increase surface tension and reduce the viscosity of the solution, and mixing of acetone and DMF would result in high fibre productivity.

PMMA/PVC: PVC is brittle and has low toughness, Chakrabarti, R. and others (Chakrabarti, R., et al., 2004) have studied the material properties of PMMA/PVC blends at 0 – 40% PMMA by dry mixing and compression molding. PMMA and PVC are compatible with each other as they have similar solubility parameters. The hardness was found to increase linearly with increasing amount of PMMA, while toughness and ductility have also increased as compared to pure PVC and peaked at 10% PMMA.

PMMA/PS: Wang, X. and others (Wang, X., et al., 2012) had used a simple spin casting method to obtain a superhydrophobic PMMA coating on glass. The surface roughness of PMMA was produced through phase separation by the means of selective solvent method. A 5 wt% mixture of PMMA and PS in the ratio of 30/70 by weight was dissolved in tetrahydrofuran (THF), and was exposed to cyclohexane to remove the PS content after spin casting, leaving behind a rough PMMA surface.

PMMA and PS are immiscible in each other although they can both be dissolved in the same solvent. Al-Kadhemy, M.F.H. and others (Al-Kadhemy, M.F.H., et al., 2017) have studied the optical characteristics for PMMA/PS blends in 0/100, 20/80, 50/50, 80/20, and 100/0 blending ratios. They found that the blends had increased UV and visible absorbance as compared to pure PMMA and PS, and 20/80 PMMA/PS reflected the most visible light.

PMMA/PVDF: PVDF is chemically inert, therefore it exhibits poor adhesion; PMMA of 20 – 30% by volume is often added into the coatings to improve scratch resistance and achieving a more glossy finish to enhance appearance (Lopez, G., et al., 2017). Aid, S. and others (Aid, S., et al., 2019) have studied the thermodynamic behavior

of PMMA/PVDF blends at different ratios of 0/100, 10/90, 30/70, 70/30, 90/10, and 100/0. They reported that the two polymers are miscible, as the crystallinity and melting temperature decreased with increasing PMMA content, at 70/30 ratio, it showed nearly no evidence of crystals. They have also studied the absorbance of the blends using Fourier-Transform Infrared (FTIR) analysis, their results showed that adding PMMA can improve visible light transmittance as compared to pure PVDF, but it would lower the IR absorbance by about half the intensity.

PMMA/PDMS: PDMS intrinsically has low chain entanglement, PMMA is usually blended in to increase the overall molecular weight to aid fabrication difficulties of PDMS alone. Ren, L. and others (Ren, L., et al., 2017) studied concentrations of PMMA in PMMA/PDMS blends and determined its effect on the hydrophobicity obtained by electrospinning. The PMMA/PDMS mixture was dissolved in equal amount of THF/DMF, a curing agent was added. They have varied the mass ratio of PMMA:PDMS for 1:2, 2:2, and 3:2, it was found that equal amount of PMMA and PDMS resulted in the highest water contact angle of 155^{o}, while higher PMMA content (145^{o}) was determined to be more hydrophobic than the coating with higher PDMS (135^{o}) content by 10^{o}.

2.2 Hydrophobicity

2.2.1 Nature inspiration

Hydrophobicity is a growing field with rising interests, it is one of the top ranked themes in material research, there were over 12,000 refereed journal publications on

superhydrophobicity, and the trend shows almost an exponential increase in number of publications in the past 10 years (Ghasemlou, M., et al., 2019). Superhydrophobic surfaces have been observed from nature in both plants and animals, such as lotus leaf, silver ragwort, and butterfly wings, which became sources of inspiration reproducing self-cleaning surfaces with different materials that mimic the same structuring found in nature (Ma, M., et al., 2008).

2.2.2 Models and criteria

Self-cleaning is a function that is categorized by the surface wetting mechanisms and is determined by the surface water contact angle (WCA). The two primary categories are hydrophobicity (repel-water) and hydrophilicity (like-water), and both are being determined by the water contact angle (WCA). The cut-off angle for the two categories is 90°, with hydrophobic > 90°, and < 90° for hydrophilic. Extent of self-cleaning is often an intrinsic property that is related to surface morphology and surface tension. (Lewin, M., et al., 2005)

Superhydrophobic (WCA > 150°) and superhydrophilic (WCA ~ 0°) can be obtained by surface modification that introduces roughness and hierarchical structures as shown in Figure 2.2. Dirt is suspended on the superhydrophobic coating that is easily carried away by water droplets, whereas superhydrophilic coating allows dirt to be readily washed away with an incoming flow of water as the dirt is embedded in the thin layer of water that forms on the coating (Son, J., et al., 2012). The related phenomenon is explained by the Cassie-Baxter model in Equation 4 (Liu, T.L., et al., 2015).

The two volume fractions f1 (rough solid) and f2 (air) sum up to unity, indicating 100% of space being occupied. θ1 and θ2 represent the contact angles of the rough solid and air, respective. To simplify the model, θ2 is approximated to be 180° assuming complete contact between the roughness and the air content. Based on the model calculations, hydrophobic surface will approach superhydrophobicity and hydrophilic surface will approach superhydrophilicity for observed contact angle θ, provided that hierarchical roughness exists. Equation 5 represents the Wenzel model which describes a more general phenomenon for when one type of roughness. When the surface is flat, the roughness factor r is one, and it follows the Young's model, demonstrated in Equation 6 which involves the surface tensions of interfaces γ; L, S, V represent liquid, solid, and vapor. The introduction of surface roughness would result in r > 1, such that the Wenzel angle θW increases when Young's angle θY is greater than 90° and decreases when θY is smaller than 90°. (Tam, J., et al., 2016)

$$\cos\theta = f1\ \cos\theta1 + f2\ \cos\theta2 \qquad (4)$$

$$\cos\theta W = r\ \cos\theta Y \qquad (5)$$

$$\gamma_{LV}\cos\theta = \gamma_{SV} - \gamma_{LS} \qquad (6)$$

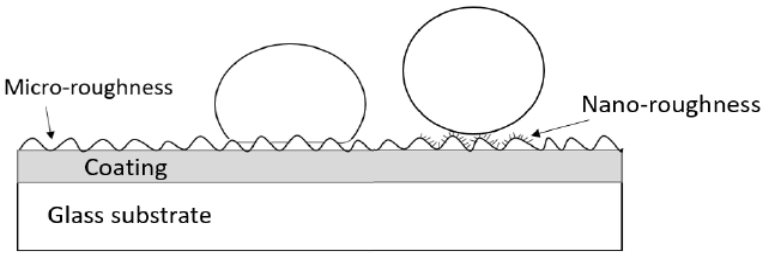

Figure 2.2. Wenzel model with micro-scale roughness (left), and Cassie-Baxter model with hierarchical roughness (right) for hydrophobic phenomena.
[Reproduced from Pao, W.Y., et al., 2019]

Texturing and sizing, together with tuning of interfacial energies are crucial to obtaining self-cleaning surfaces. Theoretically it is difficult to obtain both superhydrophobicity and transparency at the same time, as self-cleaning requires high surface roughness where the roughness would cause light scattering (Levkin, P.A., et al., 1998). Areias, C.A. and others (Areias, A.C., et al., 2012) have studied the effect of crystallinity on hydrophobicity of electrospun polylactide fibrous mat, they reported that the roughness had no significant changes with varying crystallinity, however the stiffness and rigidity crystallinity offers can greatly increase the WCA.

2.2.3 Contact angle measurements

Static water contact angle (WCA) is a standard evaluation of surface wettability, the angle is measured with respect to a flat horizontal surface as shown in Figure 2.3 (a) when the water droplet is stationary. Angle of hysteresis on the other hand characterize the advancing and receding angles. There are two main methods to measure the angle of hysteresis including tilting the surface as shown in Figure 2.3 (b), and creating expansion and shrinkage of water droplet using dispensing and sucking with a pipette as shown in Figure 2.3 (c) and (d). The tilting method can be used to determine the roll-off angle simultaneously, where the later method can avoid the need of a separate goniometer stage. (Ghasemlou, M., et al., 2019)

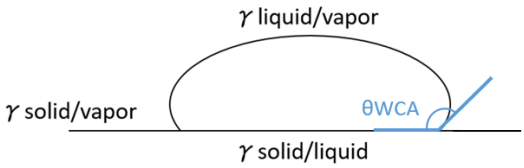

(a)

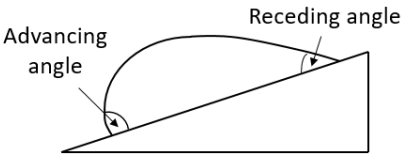

(b)

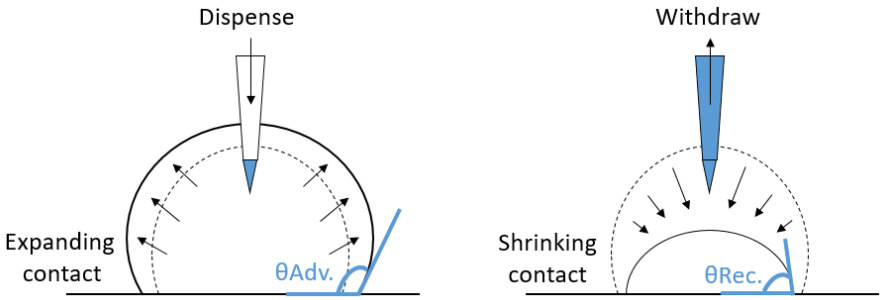

(c) (d)

Figure 2.3. Static and hysteresis water contact angle measurements.

2.2.4 Dynamic water droplet behavior

The different dynamic behaviors of water droplet on hydrophobic surfaces have been reported in literature. Bouncing, rolling, and the ability of water droplet to remove substances are the common tests. Wu, Y. and others (Wu, Y., et al., 2006) have dropped the water droplet from 3 mm in height and measured the bouncing height, the images were

captured with high speed camera during the process. They have also recorded the rolling motion of water droplet on an incline, the droplet was also dropped from 3 mm of height.

Li, Z. and others (Li, Z., et al., 2017) have studied the impact of water droplet on a few hydrophobic polymer-based surfaces that have different static WCAs ranging from 100^{o} to 160^{o}. They have captured images of the droplet behavior from 0 ms to 36 ms, where the droplet of 10 μL was dropped in free fall from 2 cm of height, the droplet bounced for the surface with close to WCA of 160^{o} while the other ones had higher affinity to the surface even for the ones that are statically superhydrophobic.

Abdelmagid, G. and others (Abdelmagid, G., et al., 2019) have investigated the effect of environmental dust particles on the water droplet dynamic behavior on a superhydrophobic surface, they have measured the droplet translational velocity on dusty surface and found that the rolling speed reduced, but evidence from 3-dimensional images showed that dust particles have been removed by the water droplet.

However, there are little to no practical tests reported in literature for the effect of hydrophobicity on water droplet behavior with respect to air speed. Very few have studied for the aerodynamic forces of the water droplet (Golpaygan, A., Ashgriz, N., 2008) (Sugioka, K., Komori, S., 2007), the onset of droplet departure (Hao, P., et al., 2013), droplet flow in a closed environment of gas flow channel (Minor, G., et al., 2009), (Hao, L., Cheng, P., 2009), and investigations of droplet deformation from a simulation perspective (Chen, K.S., et al., 2005), (Shirani, E., Masoomi, S., 2008), and (Nakata, N., et al., 2012).

2.3 Solar Irradiation and Heat Transfer

2.3.1 Solar Spectrum

Sunlight consists of three main classes of lights: ultraviolet (UV), visible light (VL), and infrared (IR); for which they lie within a specific range of wavelengths of 290 – 400 nm, 400 – 700 nm, and 700 nm – 1 mm, respectively. Each range of wavelengths contribute to a different intensity of irradiation. Figures 2.4 shows the heat distribution at sea level, the spectra indicate that both infrared (IR) and visible light contribute to most of the heat on earth, while ultraviolet (UV) contributes to only small amount although having higher energy. Although UV has the highest energy, it mostly promotes photo-degradation to objects rather than retaining as heat. (Jelle, B.P., et al., 2015) To reduce the amount of heat, it is therefore logical to develop a device that absorbs or reflects in visible and IR regions.

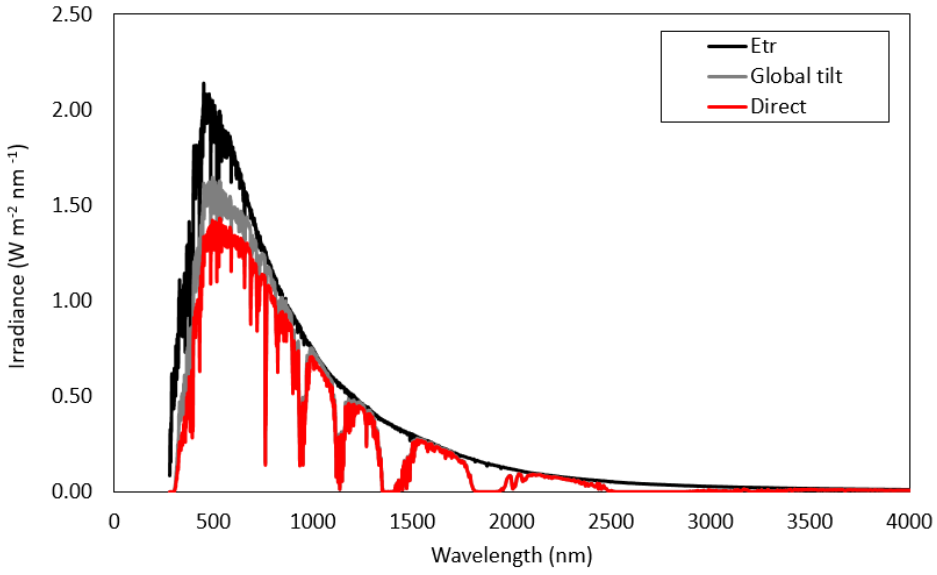

Figure 2.4. Solar irradiation spectrum showing heat distribution.
[Plot generated from data points that were retrieved from ASTM, G173-03, 2003]

2.3.2 Window heat gain and loss

The heat transfers in conventional double panes windows are primarily radiation, conduction, and secondary convection, they can be characterized by two values: solar heat gain coefficient (SHGC) and U-value which describes thermal transmittance.

SHGC is the ratio of incident solar energy on the window that reaches the inner space of the building. SHGC, as shown in Equation 7, is also known as the g-factor and can be calculated by the sum of the solar transmittance and absorbed energy which is the cause for secondary convection (Sierra, P., Hernandez, J.A., 2017). SHGC can also be measured based on heat gain of an area demonstrated in Equation 8, where Q, A, and G represent energy gain, area, and irradiance. Based on Equation 8, SHGC can be determined from the y-intercept of a plot of $(T_{indoor} - T_{outdoor})/G$ (Brunger, A., et al., 1999).

$$SHGC = g = T + A \quad (7)$$

$$SHGC = \frac{Q}{A \cdot G} \quad (8)$$

During the cold days, windows contribute to higher heat loss than walls in building structures. Since windows have high transmittance, it allows heat to enter in the hot days and heat to escape in the cold days. Thermal transmittance is quantified by U-value, the lower the U-value, the better it is for the insulation. Typical U-values for roof, external wall, floor, and windows are 0.16, 0.30, 0.25, and 2.0 W/m^2K, respectively. (Mempouo, B., et al., 2010) The U-value can be estimated from Equation 8 where U-value equals to the slope of the plot during daytime (Brunger, A., et al., 1999).

2.3.3 Films and coatings for passive climatic control

Low emissivity materials can reflect light waves instead of absorbing, low-e windows were first introduced in the market in the 1970s which are factory coated windows with either hard (inorganic) or soft (metal-based) coatings (Jelle, B.P., et al., 2015). Recently, the development of solar reflective polymer coatings are also considered to be an alternative. Xing, Z. and others (Xing, Z., et al, 2015) produced a filler-free PS coating by solution casting method, the evaporation of DMF solvent was aided with moisture condensation to promote chain contractions in PS and form grains, the coating performed better than conventional titanium dioxide coating and can reflect 70% of solar radiation.

2.4 Spray Deposition

2.4.1 Coating methods

Coatings allow a layer of material with desirable features to be adhered onto substrates, including aesthetics, protections, and special electronic functions. The curing of coatings by heat and UV or energy input is sometimes essential to create a uniform layer and effectively dry and solidify the layer. (Ryntz, R.A., Yaneff, P.V., 2003)

There are different coating and film formation methods, such as blade coating, slot-die coating, spin coating, dip coating, and spray coating. Blade coating and slot-die coating are suitable for large scale; however it forms aggregation easily when high concentration of the solution is used. Spin coating can produce uniform coating with desired thicknesses. However, the method is not very efficient with high waste contents. Dip coating is an easy

and fast process, but the drying is slow and difficult to control. Spray coating can accommodate a broad range of fluids with different viscosities, however the film might be thick with roughness. (Aziz, F., Ismail, A.F., 2015)

2.4.2 Spray coating

The spray coating process is inexpensive and has high yield, Figure 2.5 shows a schematic of the spray coating process and mechanism. Typically air, nitrogen, or other inert gas mixtures are the choices of gas. A gas stream is used to generate pressure within the spray gun, the solution is injected by gravity from the reservoir and intersects with the incoming gas stream. The stream is then atomized into wet particles and accelerate from the nozzle towards a substrate, the solvent is partially evaporated during its flight onto the substrate, and a thin film would form as thickness increases. (Aziz, F., Ismail, A.F., 2015)

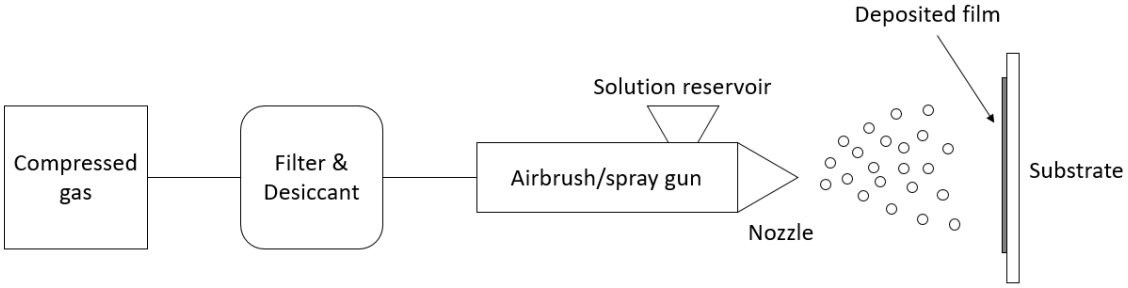

Figure 2.5. Spray coating setup and process explanation.
[Reproduced from Pao, W.Y., et al., 2019]

Spray coating is a versatile method which is compatible with different polymer solutions, Cho, Y. and others (Cho, Y., et al., 2013) have spray coated PMMA, PS, acrylonitrile butadiene (ABS), and poly(carbonate) (PC) dissolved in various solvents of

methanol, methyl chloride, and THF. Superhydrophobic coatings have been achieved with exposure to low surface energy component of trichlorosilane as post-treatment in an air tight chamber at elevated temperature.

Although the process is straightforward, the material is forced through the nozzle to form fine aerosol to be deposited on a substrate, film forms upon drying; the deposition involves different parameters that would result in different microstructures hence properties. The parameters of spray coating include distance between airbrush nozzle and the substrate, flow rate of solution, pressure of compressed gas, spray duration, number of sprayed layers, substrate temperature, and solution concentration. (Aziz, F., Ismail, A.F., 2015)

The space in between the nozzle and substrate can be divided into regions. It is wet closer to the nozzle as the aerosol is first formed, the middle region is the intermediate transition towards the dryer region at the substrate. The thickness shows linear relationship with spraying time within the intermediate zone, and the distance at which is determined to be intermediate zone depends on the solution properties. Fast drying is desired to prevent re-dissolving of the sublayers of sprayed material, however pin-holes and non-homogeneity can occur if the drying is too fast. Spray coating can create roughness through the use of mixed solvent, which is suitable to generate non-wetting surfaces which requires the surface roughness. (Aziz, F., Ismail, A.F., 2015)

2.5 References

Abdelmagid, G., Yilbas, B.S., Al-Sharafi, A., Al-Qahtani, H., and Al-Aqeeli, N., "Water droplet on inclined dusty hydrophobic surface: influence of droplet volume on environmental dust particles removal." *RSC Advances* 9, no. 7 (2019): 3582-3596.

Aid, S., Eddhahak, A., Khelladi, S., Ortega, A., Chaabani, S., and Tcharkhtchi, A., "On the miscibility of PVDF/PMMA polymer blends: Thermodynamics, experimental and numerical investigations." *Polymer Testing* 73 (2019): 222-231.

Al-Kadhemy, M.F.H., Saeed, A.A., Khaleel, R.I., and Al-Nuaimi, F.J.K., "Effect of gamma ray on optical characteristics of (PMMA/PS) polymer blends." *Journal of Theoretical and Applied Physics*11, no. 3 (2017): 201-207.

Ali, U., Karim, K.J.B.A., and Buang, N.A., "A review of the properties and applications of poly (methyl methacrylate) (PMMA)." *Polymer Reviews* 55, no. 4 (2015): 678-705.

American Society for Testing and Materials. Committee G03 on Weathering and Durability. *Standard tables for reference solar spectral irradiances: direct normal and hemispherical on 37° tilted surface*. ASTM international, 2003.

Areias, A.C., Ribeiro, C., Sencadas, V., García-Giralt, N., Diez-Perez, A., Ribelles, J.G., and Lanceros-Méndez, S., "Influence of crystallinity and fiber orientation on hydrophobicity and biological response of poly (l-lactide) electrospun mats." *Soft Matter* 8, no. 21 (2012): 5818-5825.

Aziz, F., and Ismail, A.F., "Spray coating methods for polymer solar cells fabrication: A review." *Materials Science in Semiconductor Processing* 39 (2015): 416-425.

Bhat, D.K., and Kumar, M.S., "Biodegradability of PMMA blends with some cellulose derivatives." *Journal of Polymers and the Environment* 14, no. 4 (2006): 385-392.

Borisov, B.I. and Markova, G.S., 1975. Change in properties of coatings from tacky polyvinyl chloride coatings for insulating underground pipelines. *Materials Science*, *9*(3), pp.330-332.

Brunger, A., Dubrous, F.M., and Harrison, S., "Measurement of the solar heat gain coefficient and U value of windows with insect screens." *ASHRAE Transactions* 105 (1999): 1038.

Callister, W.D., *Fundamentals of materials science and engineering*. Vol. 471660817. London, UK: Wiley, 2000.

Caruso, F., Mosca, M., Rinella, S., Macaluso, R., Calì, C., Saiano, F., and Feltin, E., "Frequency-Downconversion Stability of PMMA Coatings in Hybrid White Light-Emitting Diodes." *Journal of Electronic Materials* 45, no. 1 (2016): 682-687.

Casasola, R., Thomas, N.L., Trybala, A., and Georgiadou, S., "Electrospun poly lactic acid (PLA) fibres: effect of different solvent systems on fibre morphology and diameter." *Polymer* 55, no. 18 (2014): 4728-4737.

Chakrabarti, R., Das, M., and Chakraborty, D., "Physical, mechanical, and thermal properties of PVC/PMMA blends in relation to their morphologies." *Journal of applied polymer science* 93, no. 6 (2004): 2721-2730.

Charmondusit, K., and Seeluangsawat, L., "Recycling of poly (methyl methacrylate) scrap in the styrene–methyl methacrylate copolymer cast sheet process." *Resources, Conservation and Recycling* 54, no. 2 (2009): 97-103.

Chen, K.S., Hickner, M.A., and Noble, D.R., "Simplified models for predicting the onset of liquid water droplet instability at the gas diffusion layer/gas flow channel interface." *International Journal of Energy Research* 29, no. 12 (2005): 1113-1132.

Cho, Y., Ahn, S.H., and Lee, S., "Fabrication and analysis of PMMA, ABS, PS, and PC superhydrophobic surfaces using the spray method." *Journal of the Korean Physical Society* 63, no. 2 (2013): 218-224.

Gao, Z., Yang, L., Qin, X., Liu, K., and Gao, Y., "Preparation of semi-insulating PANI/PMMA coating and its applications in internal charging protection." *The International Journal of Advanced Manufacturing Technology* 96, no. 5-8 (2018): 1545-1552.

Ghasemlou, M., Daver, F., Ivanova, E.P., and Adhikari, B., "Bio-inspired Sustainable and Durable Superhydrophobic Materials: From Nature to Market." *Journal of Materials Chemistry A* (2019).

Golpaygan, A., and Ashgriz, N., "Multiphase flow model to study channel flow dynamics of PEM fuel cells: deformation and detachment of water droplets." *International journal of computational fluid dynamics* 22, no. 1-2 (2008): 85-95.

Hansen, C.M., *Hansen solubility parameters: a user's handbook*. CRC press, 2002.

Hao, L., and Cheng, P., "Lattice Boltzmann simulations of liquid droplet dynamic behavior on a hydrophobic surface of a gas flow channel." *Journal of Power Sources* 190, no. 2 (2009): 435-446.

Hao, P., Lv, C., and Yao, Z. "Droplet detachment by air flow for microstructured superhydrophobic surfaces." *Langmuir* 29, no. 17 (2013): 5160-5166.

Jelle, B.P., Kalnæs, S.E., and Gao, T., "Low-emissivity materials for building applications: A state-of-the-art review and future research perspectives." *Energy and Buildings* 96 (2015): 329-356.

Jones, F.N., Mark E. Nichols, and Pappas, S.P., *Organic coatings: science and technology*. John Wiley & Sons, 2017.

Kang, Y., Wang, J., Yang, G., Xiong, X., Chen, X., Yu, L., and Zhang, P., "Preparation of porous super-hydrophobic and super-oleophilic polyvinyl chloride surface with corrosion resistance property." *Applied Surface Science* 258, no. 3 (2011): 1008-1013.

Kronlund, D., Lindén, M., and Smått, J., "A polydimethylsiloxane coating to minimize weathering effects on granite." *Construction and Building Materials* 124 (2016): 1051-1058.

Levkin, P.A., Svec, F., and Fréchet, J.M., "Porous polymer coatings: a versatile approach to superhydrophobic surfaces." *Advanced functional materials*19, no. 12 (2009): 1993-1998.

Lewin, M., Mey-Marom, A., and Frank, R., "Surface free energies of polymeric materials, additives and minerals." *Polymers for advanced technologies* 16, no. 6 (2005): 429-441.

Li, Z., Kong, Q., Ma, X., Zang, D., Guan, X., and Ren, X., "Dynamic effects and adhesion of water droplet impact on hydrophobic surfaces: Bouncing or sticking." *Nanoscale* 9, no. 24 (2017): 8249-8255.

Liu, T.L., Chen, Z., and Kim, C., "A dynamic Cassie–Baxter model." *Soft Matter* 11, no. 8 (2015): 1589-1596.

Lopez, G., Guerre, M., Améduri, B., Habas, J., and Ladmiral, V., "Photocrosslinked PVDF-based star polymer coatings: an all-in-one alternative to PVDF/PMMA blends for outdoor applications." *Polymer Chemistry* 8, no. 20 (2017): 3045-3049.

Ma, M., Hill, R.M., and Rutledge, G.C., "A review of recent results on superhydrophobic materials based on micro-and nanofibers." *Journal of Adhesion Science and Technology* 22, no. 15 (2008): 1799-1817.

Mempouo, B., Cooper, E., and Riffat, S.B., "Novel window technologies and the code for sustainable homes in the UK." *International Journal of Low-Carbon Technologies* 5, no. 4 (2010): 167-174.

Minor, G., Djilali, N., Sinton, D., and Oshkai, P., "Flow within a water droplet subjected to an air stream in a hydrophobic microchannel." *Fluid dynamics research* 41, no. 4 (2009): 045506.

Nakata, N., Kakimoto, M., and Nishita, T., "Animation of water droplets on a hydrophobic windshield." (2012).

Pao, W.Y., Pop-Iliev, R., Rizvi, G., "Investigative experimental study of the wetting behavior of transparent coatings of PMMA blends with PVC/PS/PVDF/PDMS." *Proceedings of CSME-CFDSC Congress 2019,* (2019)

Peng, C., Xing, S., Yuan, Jiayu Xiao, J., Wang, C., and Zeng, J., "Preparation and anti-icing of superhydrophobic PVDF coating on a wind turbine blade." *Applied Surface Science* 259 (2012): 764-768.

Petrochenko, P.E., Zheng, J., Casey, B.J., Bayati, M.R., Narayan, R.J., and Goering, P.L., "Nanosilver-PMMA composite coating optimized to provide robust antibacterial efficacy while minimizing human bone marrow stromal cell toxicity." *Toxicology in Vitro* 44 (2017): 248-255.

Ren, L., Xia, F., Shao, J., Zhang, X., and Li, J., "Experimental investigation of the effect of electrospinning parameters on properties of superhydrophobic PDMS/PMMA membrane and its application in membrane distillation." *Desalination* 404 (2017): 155-166.

Ryntz, R.A., and Yaneff, P.V., *Coatings of polymers and plastics*. Vol. 21. CRC Press, 2003.

Schaffer, J.P., Saxena, A., Antolovich, S.D., Sanders, T.H., and Warner, S.B., *The science and design of engineering materials*. Chicago: Irwin, 1995.

Sanditov, D.S., and Razumovskaya, I.V., "New Approach to Justification of the Williams–Landel–Ferry Equation." *Polymer Science, Series A* 60, no. 2 (2018): 156-161.

TA Instruments, "Application of Time-Temperature Superposition Principles to Rheology." *Applications Notes Library*, Ref# RN011

Shirani, E., and Masoomi, S., "Deformation of a droplet in a channel flow." *Journal of fuel cell science and technology* 5, no. 4 (2008): 041008.

Sierra, P., and Hernández, J.A., "Solar heat gain coefficient of water flow glazings." *Energy and Buildings* 139 (2017): 133-145.

Son, J., Kundu, S., Verma, L.K., Sakhuja, M., Danner, A.J., Bhatia, C.S., and Yang, H., "A practical superhydrophilic self cleaning and antireflective surface for outdoor photovoltaic applications." *Solar Energy Materials and Solar Cells* 98 (2012): 46-51.

Soumya, S., Mohamed, A.P., Mohan, K., and Ananthakumar, S., "Enhanced near-infrared reflectance and functional characteristics of Al-doped ZnO nano-pigments embedded PMMA coatings." *Solar Energy Materials and Solar Cells* 143 (2015): 335-346.

Sugioka, K., and Komori, S., "Drag and lift forces acting on a spherical water droplet in homogeneous linear shear air flow." *Journal of Fluid Mechanics* 570 (2007): 155-175.

Tam, J., Palumbo, G., and Erb, U., "Recent advances in superhydrophobic electrodeposits." *Materials* 9, no. 3 (2016): 151.

Utracki, L.A., and Wilkie, C.A., *Polymer blends handbook*. Vol. 1. Dordrecht: Kluwer academic publishers, 2002.

Wang, X., Yang, N., Xu, Q., Mao, C., Hou, X., and Shen, J., "Preparation of a novel superhydrophobic PMMA surface with nanostructure and its blood compatibility." *e-Polymers* 12, no. 1 (2012).

Williams, D.J., and Amundson, N.R., *Polymer science and engineering*. Englewood Cliffs, New Jersey: Prentice-Hall, 1971.

Wu, Y., Saito, N., Nae, F.A., Inoue, Y., and Takai, O., "Water droplets interaction with super-hydrophobic surfaces." *Surface science* 600, no. 18 (2006): 3710-3714.

Xing, Z., Tay, S., Liu, Y., and Hong, L., "Solar heat reflective coating consisting of hierarchically assembled polystyrene nanoparticles." *Surface and Coatings Technology* 265 (2015): 99-105.

Zhao, Y., Zhang, Z., Yu, L., and Jiang, T., "Hydrophobic polystyrene/electro-spun polyaniline coatings for corrosion protection." *Synthetic Metals* 234 (2017): 166-174.

Zhou, X.D., and Gu, H.C., "Synthesis of PMMA-ceramics nanocomposites by spray process." *Journal of materials science letters* 21, no. 7 (2002): 577-580.

Chapter 3. Experimental

3.1 Materials

3.1.1 Polymers

The polymers used in this research include poly(methyl methacrylate) (PMMA), poly(vinyl chloride) (PVC), polystyrene (PS), poly(vinylidene difluoride) (PVDF), and poly(dimethyl siloxane) (PDMS). An important requirement of the selected polymers is transparency after being deposited on glass substrates to maintain visibility for the targeted applications of windows and windshields. The selected polymers have been reviewed in Chapter 2.1 for properties and common applications. Their chemical structures are shown in Figure 3.1.

Poly(methyl methacrylate) (PMMA) was selected to be the primary material for blending as it offers high transparency, and excellent adhesion to substrate (Ali, U., et al., 2015). PMMA is hydrophilic in nature as it has relatively high surface tension as compared to other polymers; therefore, it is hypothesized that by blending them with PMMA, the hydrophobicity of the coatings should improve. However, it can be seen that the relationship between WCA and surface tension is not linear from Table 3.1. There could be other factors which also affect the wettability of surface, such as roughness and stiffness, as discussed in Chapter 2.2, which were to be investigated in Chapter 4. The coatings produced from the selected polymers and their blends with PMMA were compared a few available products from the market, including RainX, 3M film, and NeverWet spray. Structure of decamethylcyclopentasiloxane (DMCPS), one of the major ingredients in RainX is shown in Figure 3.2.

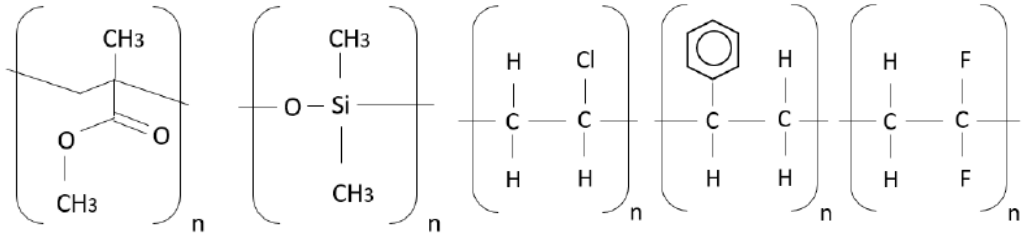

Figure 3.1. Polymer chemical structures from left to right: PMMA, PDMS, PVC, PS, and PVDF.

[Reproduced from Pao, W.Y., et al., 2019]

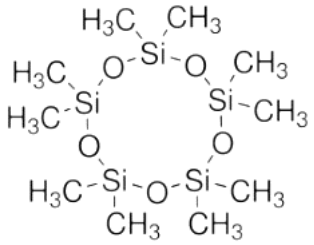

Figure 3.2 Chemical structure of decamethylcyclopentasiloxane.
[Reproduced from Sigma Aldrich Product Specification, CAS no. 541-02-6]

Table 3.1 shows the WCA and surface tensions in literature (Ma, Y., et al., 2007), (Diversified Enterprises, 2017). All polymers were used as received from Sigma Aldrich without pre-treatments, the selected grades based on weight averaged molecular weights (Mw) are also recorded in Table 3.1. High Mw grades were chosen as it has been studied by Khoryani, Z. and others (Khoryani, Z., et al., 2018) that surfaces produced from higher Mw would have an effect of increased WCA. Material properties of DMCPS that is found in RainX is also presented in Table 3.1 for reference (Wohlfarth, C.), it should be noted that DMCPS is a non-polymer entity, thus molecular weight is low.

Table 3.1. Material properties of selected polymers.

Polymer	Water contact angle (deg)	Surface tension (mN/m)	Molecular weight (g/mol)	Additional notes
PMMA	68	41	350,000	-
PVC	86	40	High Mw grade	-
PS	87	39.7	350,000	Mn ~ 170,000
PVDF	89	29.2	275,000	Mn ~ 107,000
PDMS	107	22.8	25,000	Vinyl terminated
DMCPS	-	18.3	370	non-polymer

3.2.3 Solvents

The major solvent used in this research was reagent grade N-dimethylformamide (DMF). Acetone was used in one set of experiments to determine the effect of a secondary solvent. Solutions were prepared by adding 10 mL of solvent(s) measured in a graduated cylinder into the Erlenmeyer flask that contains pre-weighted polymer powder/pellets. The solutions were stirred with a magnetic stirrer at 200 RPM and ambient temperature for 12 hours. Solubility of solutions were determined by observing homogeneous mixture without precipitates. Solubility tests of 5 wt% polymers and their blends in DMF, acetone, and at 80/20 DMF:acetone ratio were performed to determine the possibility to spray coat with the selected solvents. The Hansen solubility parameters of the polymers and solvents are shown in Table 3.2 (Hansen, C.M., 1967), (Vebber, G.C., et al., 2014), (Das, S., 2014), (Qian, L., et al., 2009), and (Rasappa, S., et al., 2018).

Table 3.2. Three-dimensional Hansen solubility parameters of polymers and solvents.

Material	Unit: $MPa^{1/2}$ δD	δP	δH	δ
DMF	17.4	13.7	11.3	24.9
Acetone	15.5	10.4	7.0	19.9
PMMA	18.6	10.5	7.5	22.6
PVC	18.2	7.5	8.3	21.4
PS	21.3	5.8	4.3	22.5
PVDF	17.2	12.5	9.2	23.2
PDMS	15.9	0.0	4.1	16.4

3.2 Spray Coating Setup and Parameters

3.2.1 Spray coating setup

The setup was built in-house with an enclosure box of 12” deep x 12” tall x 18” wide in dimensions. The substrate holder is placed in the center and the location can be adjusted for different distances from the nozzle tip of the spray gun, the measuring guide for spray distances is taped at the bottom of the box. The spray gun rests on a rail for left and right movements to ensure uniform coating and prevents concentrated deposition on certain spots. A desk lamp is placed inside the enclosure box to maintain ambient temperature of 30°C during the spray process, a timer is used to measure spray time and the speed of spray gun movements.

The spray coating setup as shown in Figure 3.3 is comprised of five main components: compressed gas source, filtering system, dual trigger spray gun, gravity feed

solution reservoir, nozzle, and target substrate. The compressed air was filtered and dehydrated through cottons and desiccants to remove impurities.

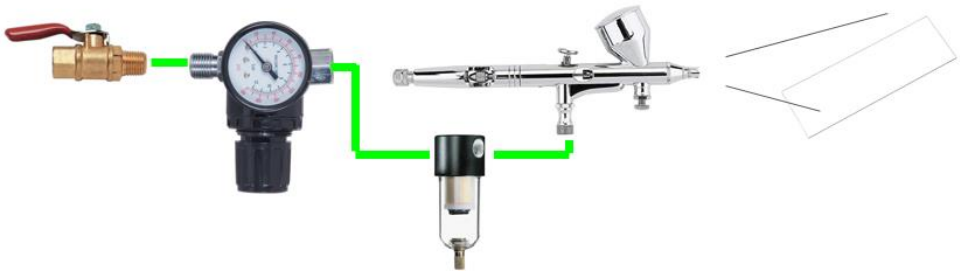

Figure 3.3. Spray coating setup.

3.2.2 Experimental Parameters Consideration

Several parameters/conditions were investigated in this research: distance from nozzle tip to substrate, compressed air pressure, solution blend formulation, and solvent used. The full sets of experiments with different parameters and conditions performed in this research are presented in Table 3. There were a total of 40 samples produced including the ones stated below and the three market products that are introduced in Chapter 1.2 such as RainX, 3M film, and NeverWet spray. Additionally, pre-cleaned uncoated glass slide purchased from AmScope was used as the control.

Spray distance and pressure are likely to have an effect on transparency and the resulting microstructure as they affect the wetness of the as deposited layer. Generally, moderate drying rate and larger microstructure would result in higher transparency, however the self-cleaning ability might be reduced, and the combination of parameters requires optimization to obtain both properties. Concentration of 5 wt% was held constant

for all solutions as it was found to be favorable for the spray coating technique with polymers.

Table 3.3. Experimental parameters.

Material	Spray conditions				
	Formulation	Pressure	Distance	Concentration	Solvent
PMMA	100/0	20	15	5	DMF
PolymerBlends	80/20	20	15	5	DMF
	50/50	20	15	5	DMF
	50/50	20	15	5	DMF/Acetone (80:20)
	50/50	20	17.5	5	DMF
	50/50	20	20	5	DMF
	50/50	15	15	5	DMF
	50/50	25	15	5	DMF
	20/80	20	15	5	DMF
Other polymers	0/100	20	15	5	DMF

3.3 Experiments

3.3.1 Solvent evaporation rate

The evaporation rates of solvents were determined by thermogravimetric analysis (TGA) by TA Instruments, the equipment is shown in Figure 3.4. The mass change of solvent was measured at isothermal condition at 30℃ as used in the spraying process.

DMF was found to evaporate slowly at close to 1.0% per minute, whereas acetone alone is extremely volatile and evaporated 24.5 times faster than DMF. Mixing of the two solvents was found to have three stages of evaporation s shown in Table 3.4.

Figure 3.4 Thermogravimetric Analysis Equipment (Q50) by TA Instruments.

Table 3.4. Evaporation rates of solvents determined by TGA.

Material	Evaporation rate
DMF	0.99 %/min
Acetone	24.31 %/min
DMF/Acetone (50/50)	3.86, 2.30, 0.92 %/min

3.3.2 Polymer coatings procedure

Sample preparation procedure:

Concentration of 5 wt% of PMMA powder (0.472 g) was measured using high precision balance scale. The measured polymer powder and pellets were dissolved in 10 mL of DMF (9.44 g) in an Erlenmeyer flask. For the solutions that contain mixed solvents of DMF and acetone, 8 mL of DMF and 2 mL of acetone were measured and were added to the flask that contained the weighted polymer(s). The solution was stoppered and let stir by a magnetic stirrer at 200 RPM for 12 hours to ensure homogeneous solution. A compressed air was run through and pressure was pre-set with a regulator before spraying.

Target substrate of 1” x 3” in size and 0.8 – 1.0 mm thick was mounted onto the spraying stage at a predetermined distance and height.

The enclosure temperature was maintained at 30℃ by the use of a lamp. The solution was then poured into the reservoir of the spray-gun and ready to be sprayed. During the spraying process, the spray gun moved left and right for 5 times each at a constant speed of 1 seconds in each direction, the coating was let dry for 1 minute in air. This process was repeated for 10 times. The sample was then cured by heat treatment on hot plate at 40°C for 10 minutes.

Concentration calculation example:

Total weight of mixed solvents = 8 mL x 0.944 g/mL + 2 mL x 0.784 g/mL = 9.12 g

Weight of 5 wt% polymers = 0.05 x 9.12 g = 0.456 g

Weight of each polymer in 50/50 blend ratio = 0.5 x 0.456 g = 0.228 g

3.4 Characterizations

3.4.1 Solar Transmittance

Solar Film Transmission meter LS182 by Linshang Technology (CNIPA Patent: 201320406828, 2013) as shown in Figure 3.5 was used to measure the transmittance and rejection of UV, IR, and visible light. The peak wavelengths of the equipment for UV, IR, and visible light are 365, 950/1400, and 550 nm, respectively. Solar heat gain coefficient (SHGC) could also be determined simultaneously.

Figure 3.5 Transmission meter LS182 by Linshang Technology, China, +/- 2% accuracy.

3.4.2 Microstructure Observations and Static Water Contact Angle Measurements

Digital optical microscope by Keyence was employed to evaluate both the microstructure and the static water contact angles (WCAs). The structure and the water droplet were visualized with the lens VH-Z100R at 100x magnification and VH-Z20R at 20x magnification, respectively. The microscope system is shown in Figure 3.6 (a), and Figure 3.6 (b) shows the ability of the free-angle observation stage VHX-S50 to be tilted to up to 90°. The images of water droplet were captured at 90° where the view of the lens was parallel to the sample stage. WCA was measured with the measurement tools of the automatic self-calibrated operation module.

(a) (b)

Figure 3.6. Keyence digital microscope VHX-1000.

3.4.3 Dynamic Water Droplet Behavior

The dynamic water droplet behavior was an important characterization that it aimed to simulate a more realistic environment of the windshield of a moving vehicle, or a surface with parallel wind. The measurement setup is shown in Figure 3.7. Compressed air was used to create the wind condition through an inlet cup that produces enlarged air flow field around the sample. The speed was controlled by the pressure regulator and was measured at the region immediately in front of the glass slide by an anemometer. It should be noted that Hao, P. and others (Hao, P., et al., 2013) have also built a similar setup to determine the onset of droplet departure from an aerodynamic perspective, however the rolling motion was not discussed.

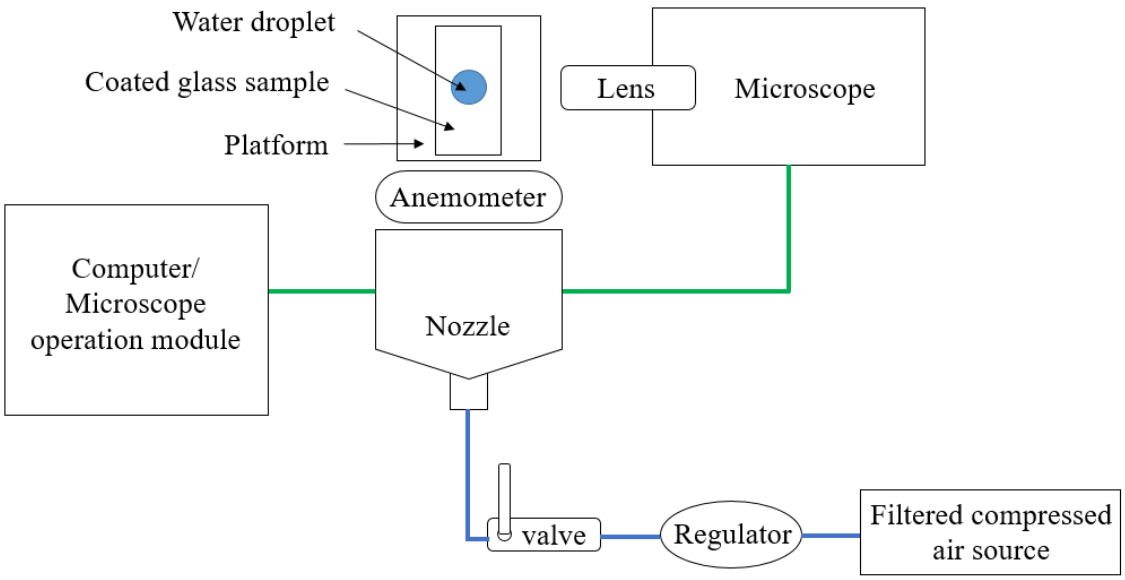

Figure 3.7 Dynamic water behavior measurement setup.

The maximum pressure output from the in-house compressed airlines was 80 psi, the corresponding maximum wind speed was measured to be 50 km/hr. The dynamic

behavior such as onset of water droplet departure with respect to speed, the rolling velocity, and the angles of hysteresis were captured using the video recording function of the Keyence microscope at 28 frames per second.

Two sets of samples were selected for the dynamic test including the pure polymers and the 50/50 blends sprayed by the reference conditions of 20 psi pressure and 15 cm distance. These samples were believed to best represent the influence of materials on the water droplet behavior. The sample was mounted on either a flat stage representing 0^o, or an inclined stage at 30^o, which is the typical angle for most windshields in modern cars. A water droplet of 5.5 μL volume was dispensed onto the sample, the wind speed was then slowly cranked up by turning the regulator and the behavior of droplet was recorded.

Experimental relationship between the droplet volume in the range of 0.5 μL to 10 μL and size in diameter (mm) is shown in Figure 3.8. Volume of 5.5 μL corresponded to about 2.5 mm in diameter, and it was the start of a stable linear relationship of droplet size.

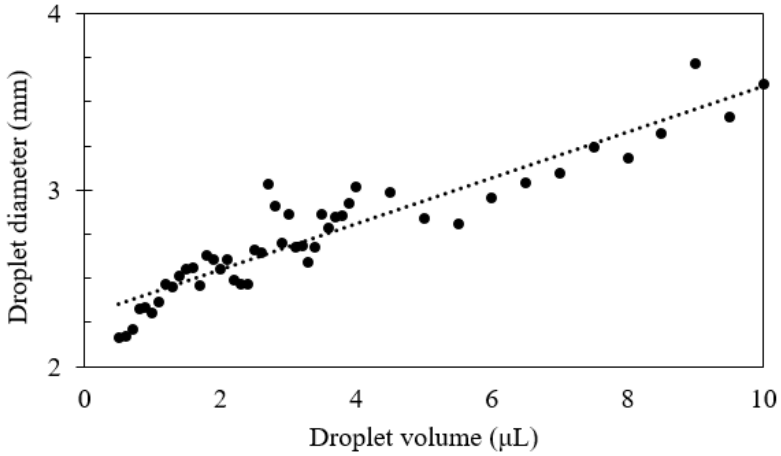

Figure 3.8. Relationship between droplet volume and size in diameter.

3.5 References

Ali, U., Karim, K.J.B.A., and Buang, N.A., "A review of the properties and applications of poly (methyl methacrylate) (PMMA)." *Polymer Reviews* 55, no. 4 (2015): 678-705.

Cohen, N., Dotan, A., Dodiuk, H., and Kenig, S., "Superhydrophobic coatings and their durability." *Materials and Manufacturing Processes* 31, no. 9 (2016): 1143-1155.

Das, S. "Solvents: properties, solubility parameter, solvation, toxicity, safety." (2014).

Diversified Enterprises, "Critical surface tension and contact angle with water for various polymers." (2016).

Hansen, C.M., "The three dimensional solubility parameter." *Danish Technical: Copenhagen* 14 (1967).

Hao, P., Lv, C., and Yao, Z., "Droplet detachment by air flow for microstructured superhydrophobic surfaces." *Langmuir* 29, no. 17 (2013): 5160-5166.

Khoryani, Z., Seyfi, J., and Nekoei, M., "Investigating the effects of polymer molecular weight and non-solvent content on the phase separation, surface morphology and hydrophobicity of polyvinyl chloride films." *Applied Surface Science* 428 (2018): 933-940.

Li, Q., Xu, Z., and Yu, L., "Effects of mixed solvents and PVDF types on performances of PVDF microporous membranes." *Journal of applied polymer science*115, no. 4 (2010): 2277-2287.

Ma, Y., Cao, X., Feng, X., Ma, Y., and Zou, H., "Fabrication of super-hydrophobic film from PMMA with intrinsic water contact angle below 90." *Polymer* 48, no. 26 (2007): 7455-7460.

Pao, W.Y., Pop-Iliev, R., Rizvi, G., “Investigative experimental study of the wetting behavior of transparent coatings of PMMA blends with PVC/PS/PVDF/PDMS.” *Proceedings of CSME-CFDSC Congress 2019,* (2019)

Rasappa, S., Schulte, L., Borah, D., Hulkkonen, H., Ndoni, S., Salminen, T., Senthamaraikanan, R., Morris, M.A., and Niemi, T., "Morphology evolution of PS-b-PDMS block copolymer and its hierarchical directed self-assembly on block copolymer templates." *Microelectronic Engineering* 192 (2018): 1-7.

Sigma-Aldrich, “Product Specification: Decamethylcyclosiloxane, Product number 444278” www.sigma-aldrich.com

Vebber, G.C., Pranke, P., and Pereira, C.N., "Calculating Hansen solubility parameters of polymers with genetic algorithms." *Journal of Applied Polymer Science* 131, no. 1 (2014).

Wohlfarth, C. "Surface tension of decamethylcyclopentasiloxane." In *Surface Tension of Pure Liquids and Binary Liquid Mixtures*, pp. 10-10. Springer, Berlin, Heidelberg, 2016.

Chapter 4. Results and Discussions

4.1 Transmittance

4.1.1 Effect of post-heat treatment

The transmittance of as received non-coated and pre-cleaned glass slide was first measured and was used as a baseline reference piece. The transmittance for the coated samples were expected to have higher or equal amount of UV/IR rejections and lower visible light (VL) transmission than bare glass. The UV rejection, IR rejection, visible light transmission, and SHGC of the uncoated glass were measured to be 10.6%, 10.8%, 91.4%, and 0.904, respectively.

Table 4.1 shows the transmittance and SHGC of 5 wt% of pure PMMA and its blends at 50/50 weight ratio, the spray conditions were 20 psi and 15 cm. The set of samples were sprayed as received without pre- and post-treatment of heating and was let dry in air. PMMA/PDMS was found to have the least protection from solar radiation as the transmittance was comparable to that of glass. PMMA/PVDF on the other hand had the lowest transparency, in turn it provided the most protection towards solar heat. Both PMMA/PVC and PMMA/PS performed similarly in terms of IR rejection, but the higher UV rejection of PMMA/PVC led to a reduced VL transmittance, overall the SHGC was only differ by 0.039. PMMA was found to behave opposite to its blends with PVC and PS, where it shields IR better than UV while maintaining similar transparency; the resulting SHGC was similar.

Table 4.1. Transmittance of PMMA and its 50/50 blends w/o post-heat treatment.

Material	UV rej	IR rej	VL trans	SHGC
PMMA	16.2 ± 0.15	21.9 ± 0.35	81 ± 0.36	0.804 ± 0.002
PMMA/PVC	27.2 ± 0.14	16.9 ± 0.34	78.2 ± 0.22	0.798 ± 0.002
PMMA/PS	19.2 ± 0.28	16.9 ± 0.38	83.5 ± 0.27	0.837 ± 0.004
PMMA/PVDF	38.5 ± 0.25	36 ± 0.41	48.5 ± 0.29	0.544 ± 0.004
PMMA/PDMS	10.5 ± 0.13	12.3 ± 0.15	92.2 ± 0.14	0.905 ± 0.001

Table 4.2 shows the same materials of 5 wt% PMMA and its blends with the reference spray conditions, heat treatment at 40°C to cure the coating has been performed immediately after the 10 x 10 layers of sprays. PMMA was found to behave similarly to uncoated glass after being heated, by mixing with a second polymer, the solar heat gain reduced in the order from the least effective: PDMS, PVC, PVDF, and PS. Post-heat treatment was found to be beneficial in aiding solvent evaporation and producing a more uniformly coated surface. In general, heat treatment has caused a more regular trend for the ranking and lower standard deviations (S.D.), it has also significantly improved the UV blockage of PS and the transparency of PVDF. Although not mandatory, it is recommended that post-heat treatment to be performed in order to ensure complete drying of coating within a short period of time to ensure better quality of final product.

Table 4.2. Transmittance of PMMA and its 50/50 blends w/ post-heat treatment.

Material	UV rej	IR rej	VL trans	SHGC
PMMA	11.7 ± 0.01	11.3 ± 0.04	90.9 ± 0.27	0.901 ± 0.001
PMMA/PVC	14.8 ± 0.12	15.9 ± 0.18	87.4 ± 0.18	0.861 ± 0.002
PMMA/PS	48.5 ± 0.25	29.4 ± 0.19	64.6 ± 0.21	0.664 ± 0.002
PMMA/PVDF	45.5 ± 0.23	19.4 ± 0.19	72.1 ± 0.20	0.747 ± 0.002
PMMA/PDMS	10.6 ± 0.11	13.7 ± 0.09	91 ± 0.12	0.892 ± 0.001

4.1.2 Effect of spray conditions

The effect of spray distances on solar transmittance is reflected in Figure 4.1 and Table 4.3, the distances were changed from the reference 15 cm to 20 cm at 2.5 cm increment, and all samples have undergone post-heat treatment. It was previously discussed in Chapter 2.4 that the drying of coating is dependent on the spray parameters, a shorter spray distance will result in a wet coating and would probably result in a less solidified layer.

It was observed that varying the spray distances had no apparent effects for PMMA and PMMA/PDMS, where the transmittance values remained relatively the same. Increasing the spray distance had caused PVDF to become more transparent, and had higher impact on altering the UV protection negatively, thus the overall heat gain increased. Based on the observations, it can be concluded that UV transmittance has a higher impact than IR on VL transparency, as its range of wavelengths are much closer to the VL region. PMMA/PVC and PMMA/PS was found to behave oppositely with the change in spray distance, when PMMA/PVC could reduce the heat gain, PMMA/PS would have a gain.

The effect of spray pressures on solar transmittance is reflected in Figure 4.2 and Table 4.4, the pressures were investigated at a lower (15 psi) and a higher value (25 psi) with respect to the reference value of 20 psi. All samples have also undergone post-heat treatment. PMMA, PMMA/PDMS, and PMMA/PVC were not sensitive to the spraying pressures as there were no significant changes and apparent trends seen. PMMA/PS and PMMA/PVDF were found to be affected by the change in spray pressures. With increasing pressure, VL transmission of PMMA/PS reduced by 12% and had a huge gain in SHGC by

20% as there were drastic changes in UV and IR rejection. PMMA/PVDF on the other hand was only affected for UV protection slightly.

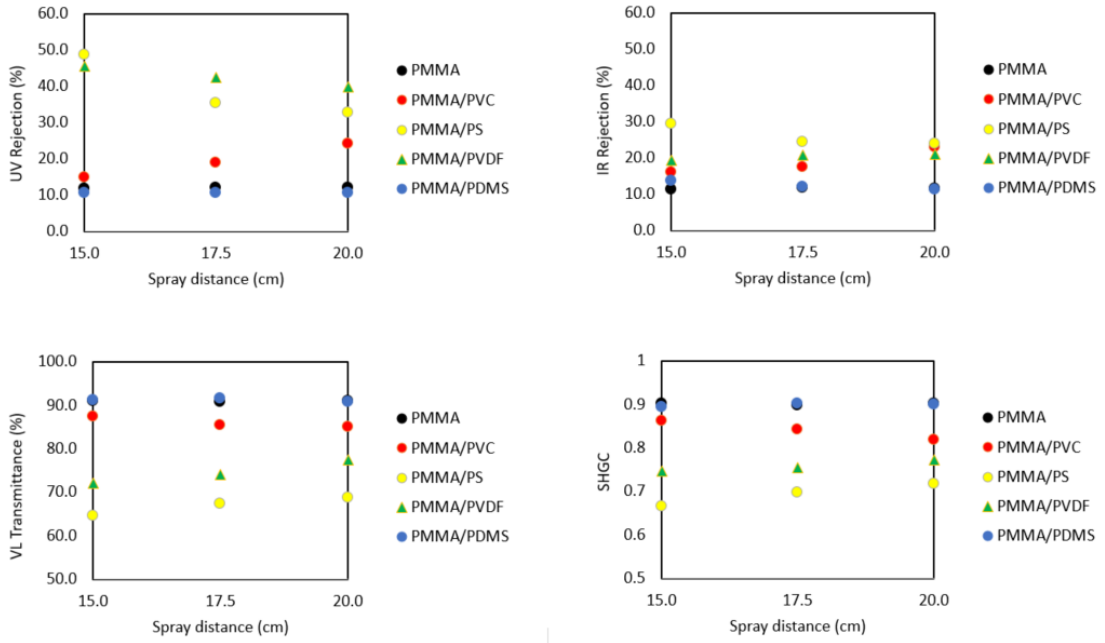

Figure 4.1. Effect of spray distance on transmittance of polymer blends. [S.D. < 0.30]

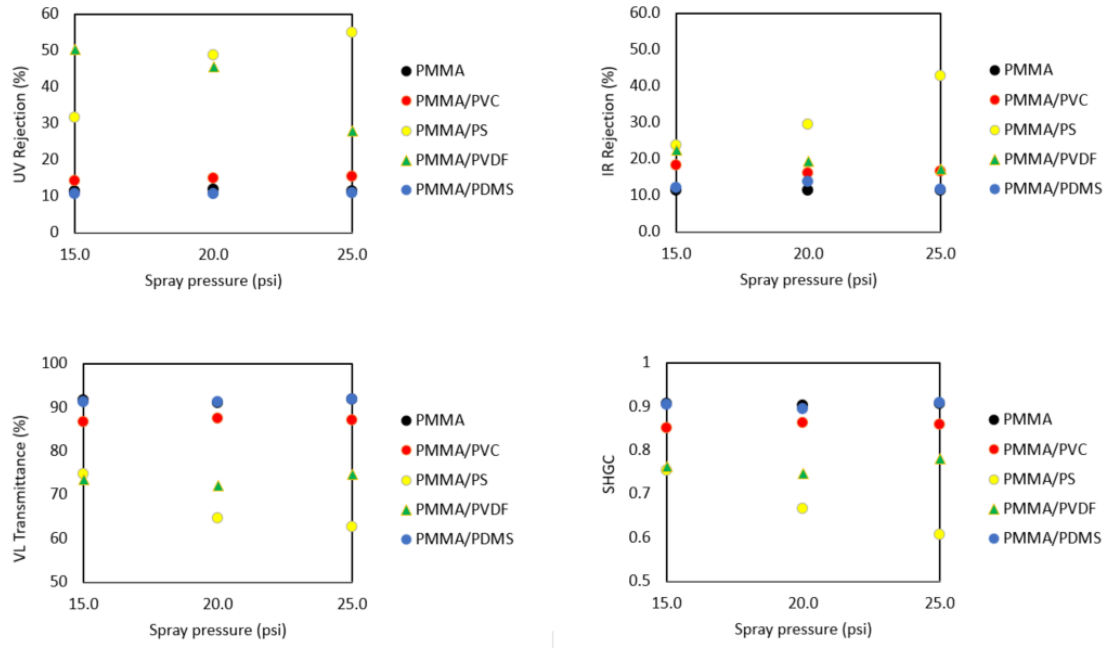

Figure 4.2. Effect of spray pressure on transmittance of polymer blends. [S.D. < 0.34]

Table 4.3. Transmittance of PMMA and its 50/50 blends at different spray distances.

Material	Distance (cm)	UV rej	IR rej	VL trans	SHGC
PMMA	15.0	11.7 ± 0.01	11.3 ± 0.04	90.9 ± 0.27	0.901 ± 0.001
PMMA	17.5	12.0 ± 0.05	11.8 ± 0.10	90.6 ± 0.25	0.897 ± 0.001
PMMA	20.0	11.9 ± 0.07	11.4 ± 0.09	90.8 ± 0.22	0.900 ± 0.001
PMMA/PVC	15.0	14.8 ± 0.12	15.9 ± 0.18	87.4 ± 0.18	0.861 ± 0.002
PMMA/PVC	17.5	18.8 ± 0.11	17.5 ± 0.15	85.3 ± 0.18	0.841 ± 0.002
PMMA/PVC	20.0	24.1 ± 0.12	22.8 ± 0.19	85.0 ± 0.16	0.817 ± 0.002
PMMA/PS	15.0	48.5 ± 0.25	29.4 ± 0.19	64.6 ± 0.21	0.664 ± 0.002
PMMA/PS	17.5	35.3 ± 0.22	24.2 ± 0.21	67.3 ± 0.21	0.696 ± 0.002
PMMA/PS	20.0	32.7 ± 0.29	23.8 ± 0.20	68.6 ± 0.20	0.716 ± 0.002
PMMA/PVDF	15.0	45.5 ± 0.23	19.4 ± 0.19	72.1 ± 0.20	0.747 ± 0.002
PMMA/PVDF	17.5	42.5 ± 0.25	20.7 ± 0.21	74.1 ± 0.19	0.755 ± 0.002
PMMA/PVDF	20.0	39.8 ± 0.30	21.0 ± 0.23	77.3 ± 0.16	0.772 ± 0.002
PMMA/PDMS	15.0	10.6 ± 0.11	13.7 ± 0.09	91.0 ± 0.12	0.892 ± 0.001
PMMA/PDMS	17.5	10.5 ± 0.12	12.0 ± 0.10	91.5 ± 0.09	0.901 ± 0.001
PMMA/PDMS	20.0	10.6 ± 0.11	11.3 ± 0.10	90.6 ± 0.08	0.899 ± 0.001

Table 4.4. Transmittance of PMMA and its 50/50 blends at different spray pressures.

Material	Pressure (psi)	UV rej	IR rej	VL trans	SHGC
PMMA	15.0	11.3 ± 0.01	11.3 ± 0.02	91.4 ± 0.15	0.904 ± 0.001
PMMA	20.0	11.7 ± 0.01	11.3 ± 0.04	90.9 ± 0.27	0.901 ± 0.001
PMMA	25.0	11.2 ± 0.01	11.3 ± 0.04	91.6 ± 0.20	0.905 ± 0.001
PMMA/PVC	15.0	14.0 ± 0.16	18.1 ± 0.16	86.5 ± 0.14	0.85 ± 0.002
PMMA/PVC	20.0	14.8 ± 0.12	15.9 ± 0.18	87.4 ± 0.18	0.861 ± 0.002
PMMA/PVC	25.0	15.3 ± 0.15	16.4 ± 0.16	86.9 ± 0.13	0.857 ± 0.002
PMMA/PS	15.0	31.5 ± 0.22	23.6 ± 0.21	74.7 ± 0.20	0.753 ± 0.002
PMMA/PS	20.0	48.5 ± 0.25	29.4 ± 0.19	64.6 ± 0.21	0.664 ± 0.002
PMMA/PS	25.0	54.8 ± 0.25	42.7 ± 0.20	62.5 ± 0.23	0.605 ± 0.002
PMMA/PVDF	15.0	50.2 ± 0.24	22.4 ± 0.25	73.5 ± 0.22	0.763 ± 0.002
PMMA/PVDF	20.0	45.5 ± 0.23	19.4 ± 0.19	72.1 ± 0.20	0.747 ± 0.002
PMMA/PVDF	25.0	27.9 ± 0.31	17.1 ± 0.34	74.7 ± 0.30	0.779 ± 0.003
PMMA/PDMS	15.0	10.4 ± 0.15	12.0 ± 0.11	91.0 ± 0.13	0.903 ± 0.001
PMMA/PDMS	20.0	10.6 ± 0.11	13.7 ± 0.09	91.0 ± 0.12	0.892 ± 0.001
PMMA/PDMS	25.0	10.7 ± 0.10	11.5 ± 0.07	91.6 ± 0.09	0.906 ± 0.001

4.1.3 Effect of formulation

The effect of formulation with different blending ratios was investigated and the transmittance for each formula is reported in Figure 4.3 and Table 4.5. The difference in formulations was found to have huge impact on most blends except for PMMA/PDMS. All other blends have obtained about 40 – 50% reduction in SHGC with lower PMMA content from 80% PMMA to pure polymer coating without PMMA. All of them were observed to have the same trend of reduced VL transmission, and increased UV/IR rejections. This suggests that PMMA is beneficial for retaining transparency for window and windshield applications, whereas the addition of secondary polymers would aid shielding for solar radiation.

There were non-linear changes observed for PMMA/PS for UV and IR protections, it was seen that UV rejections remained relatively constant from 0 – 50% PMMA content, however there was a large reduction in UV protection as PS content was reduced to 20%. This could be due to the immiscibility of PMMA and PS, such that at 80/20 PMMA/PS the performance of the coated surface resembles more of pure PMMA rather than following the rule of mixture.

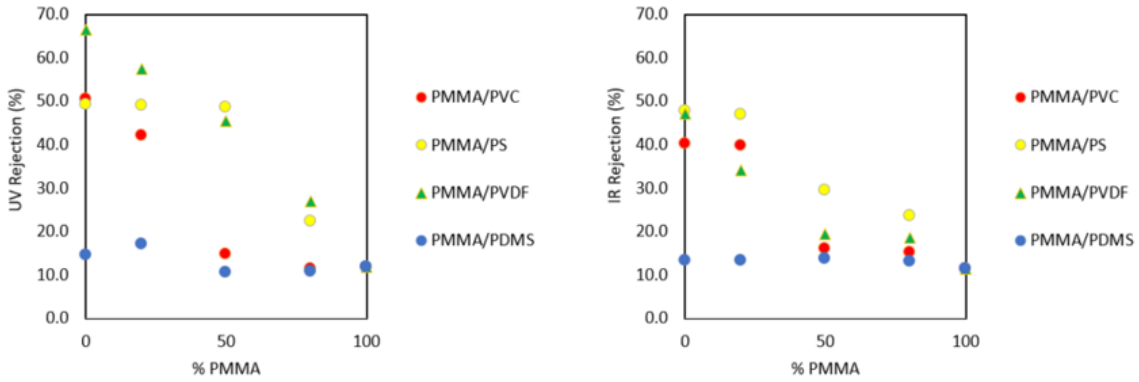

(a) (b)

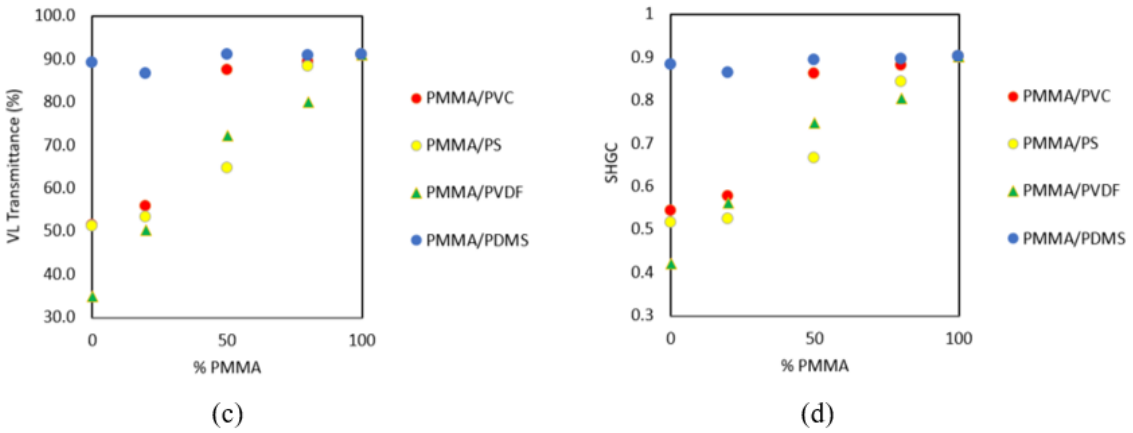

(c) (d)

Figure 4.3. Effect of formulation on transmittance of polymer blends. [S.D. < 0.35]

Table 4.5. Transmittance of PMMA blends at different blending ratios.

Material	Blend ratio	UV rej	IR rej	VL trans	SHGC
PMMA/PVC	80/20	11.3 ± 0.15	15.2 ± 0.15	89.3 ± 0.15	0.879 ± 0.001
	50/50	14.8 ± 0.12	15.9 ± 0.18	87.4 ± 0.18	0.861 ± 0.002
	20/80	42.0 ± 0.16	39.8 ± 0.16	55.8 ± 0.17	0.577 ± 0.002
	0/100	50.5 ± 0.10	40.2 ± 0.08	51.4 ± 0.10	0.543 ± 0.001
PMMA/PS	80/20	22.3 ± 0.22	23.6 ± 0.21	88.2 ± 0.18	0.842 ± 0.002
	50/50	48.5 ± 0.25	29.4 ± 0.19	64.6 ± 0.21	0.664 ± 0.002
	20/80	49.0 ± 0.31	46.8 ± 0.35	53.3 ± 0.27	0.523 ± 0.003
	0/100	49.1 ± 0.21	47.8 ± 0.19	51.1 ± 0.19	0.515 ± 0.001
PMMA/PVDF	80/20	26.9 ± 0.21	18.5 ± 0.20	80.0 ± 0.18	0.804 ± 0.002
	50/50	45.5 ± 0.23	19.4 ± 0.19	72.1 ± 0.20	0.747 ± 0.002
	20/80	57.4 ± 0.29	34.1 ± 0.30	50.2 ± 0.30	0.562 ± 0.003
	0/100	66.5 ± 0.20	47.0 ± 0.22	34.9 ± 0.20	0.420 ± 0.002
PMMA/PDMS	80/20	10.8 ± 0.08	13.0 ± 0.11	90.7 ± 0.07	0.895 ± 0.001
	50/50	10.6 ± 0.11	13.7 ± 0.09	91.0 ± 0.12	0.892 ± 0.001
	20/80	17.1 ± 0.15	13.3 ± 0.16	86.5 ± 0.15	0.864± 0.002
	0/100	14.5 ± 0.08	13.3 ± 0.10	89.1 ± 0.09	0.882 ± 0.001

4.1.4 Effect of solvent

The transmittance of coatings made from one-solvent (DMF) and two-solvents (DMF + Acetone) systems are compared in Table 4.6. The polymers were blended at 50/50 ratio, and sprayed with the reference parameters. With the introduction of acetone, full UV protection was made possible and a minimum 35% improvement in IR rejection, thus very low SHGCs were achieved, however at the expense of visible transparency.

The drying of the coating is highly dependent on the evaporation rate of solvent, solvents with low vapor pressures such as DMF tend to evaporate slower, whereas solvents with high vapor pressures such as acetone leave the coating quickly. The fast evaporation of acetone can cause undesired condensation and whitening of the drying film, thus it should not be used as the primary solvent and should be used only in small amount to retain transparency. Besides, the evaporation rates of this mixed solvent system was previously determined to be non-linear, causing difficulty in predicting and controlling the transmittance.

Table 4.6. Transmittance of coatings prepared from different solvent systems.

Material	Solvent	UV rej	IR rej	VL trans	SHGC
PMMA	DMF	11.7 ± 0.01	11.3 ± 0.04	90.9 ± 0.27	0.901 ± 0.001
	DMF/Ace 80/20	98.0 ± 0.14	91.9 ± 0.17	3.30 ± 0.18	0.051 ± 0.002
PMMA/PVC	DMF	14.8 ± 0.12	15.9 ± 0.18	87.4 ± 0.18	0.861 ± 0.002
	DMF/Ace 80/20	73.7 ± 0.23	52.5 ± 0.24	32.5 ± 0.32	0.378 ± 0.003
PMMA/PS	DMF	48.5 ± 0.25	29.4 ± 0.19	64.6 ± 0.21	0.664 ± 0.002
	DMF/Ace 80/20	99.5 ± 0.36	83.2 ± 0.31	1.40 ± 0.13	0.069 ± 0.004
PMMA/PVDF	DMF	45.5 ± 0.23	19.4 ± 0.19	72.1 ± 0.20	0.747 ± 0.002
	DMF/Ace 80/20	96.3 ± 0.32	61.5 ± 0.33	7.20 ± 0.30	0.188 ± 0.004
PMMA/PDMS	DMF	10.6 ± 0.11	13.7 ± 0.09	91.0 ± 0.12	0.892 ± 0.001
	DMF/Ace 80/20	85.3 ± 0.15	51.0 ± 0.16	22.7 ± 0.12	0.327 ± 0.002

4.1.5 Product comparison

A few fabricated coatings were selected to compare with the available market products for the transmittance, including PMMA and PDMS, their values are presented in Table 4.7. PMMA is the material that is the most comparable to bare uncoated glass, and is the focus of this research to evaluate the probability to utilize PMMA as coating material for windows and windshields. RainX contains decamethylcyclopentasiloxane, which also belongs to the same silicone group as PDMS, and NeverWet formulation contains acetone, however the other ingredients are not disclosed by the company.

Table 4.7. Transmittance of market products and selected fabricated coatings.

Material	UV rej	IR rej	VL trans	SHGC
Glass	10.6 ± 0.01	10.8 ± 0.02	91.4 ± 0.03	0.904 ± 0.000
RainX	11.0 ± 0.10	11.6 ± 0.10	90.8 ± 0.08	0.900 ± 0.001
3M	21.4 ± 0.07	19.5 ± 0.07	82.0 ± 0.05	0.816 ± 0.001
NeverWet	95.0 ± 0.12	63.3 ± 0.15	26.4 ± 0.07	0.295 ± 0.001
100% PMMA	11.7 ± 0.01	11.3 ± 0.04	90.9 ± 0.27	0.901 ± 0.001
PMMA/PDMS in DMF	10.6 ± 0.11	13.7 ± 0.09	91.0 ± 0.12	0.892 ± 0.001
100% PDMS	14.5 ± 0.08	13.3 ± 0.10	89.1 ± 0.09	0.882 ± 0.001
PMMA/PDMS in DMF/Acetone	85.3 ± 0.15	51.0 ± 0.16	22.7 ± 0.12	0.327 ± 0.002

It is observed that both RainX and PMMA are almost identical in transmittance, both of them have high VL transmittance which can be confidently used on glasses that requires transparency. Blending PMMA with PDMS can slightly improve the IR rejection and bring down the SHGC by 0.08. 100% PDMS might seem to be a suitable alternative as it offers higher UV and IR protection while maintaining high enough transparency, however, due to the low surface energy, it might not adhere well on the glass surface without PMMA and will lead to durability issues.

NeverWet although is extremely superior in water repellency, it sacrifices the transparency and is not suitable for see-through applications, the same was observed in PMMA/PDMS prepared from DMF/Acetone in 80:20 combination. Lastly, the exterior 3M insulator film claims to be heat insulating during the cold days, it was therefore tested to assist with the understanding the relationship between solar transmittance and prevention of heat loss. It was found to be able to reject UV and IR to a better extent than the compared transparent coatings.

4.2 Microstructure

4.2.2 Effect of polymer chemical groups

Microstructure of 5 wt% pure polymer coatings prepared in DMF with reference spray parameters and post-heat treatment is shown in Figure 4.4. The effect of different microstructure had caused differences in visible light transmittance, i.e. transparency. It is known that roughness and grain-like structures can deflect light, thus lowering the transparency. Both PMMA and PDMS (Figure 4.4 (a) and (b)) achieved transparency comparable to bare glass slide, as it is evident that both polymers are amorphous and the coatings were smooth. The bands formed in PMMA could be due to the spraying process when new layers have deformed the previous layers that were not fully dried.

PS and PVC were found to have the same VL transmittance, although PS has larger microstructural size than PVC as shown in the comparison between Figure 4.4 (c) and (d), the shapes were observed to be similar. That could be due to the fact that the similarity in molecular structure for the two polymers, differing only by one substituent of Cl and

benzene ring. The benzene ring is likely to be larger in size than the chlorine atom, therefore more amorphous regions can be found in PS than PVC.

The grain-like structure in both PS and PVC might just be aggregates rather than crystals where the first seems to be more probable as both PVC and PS are known to be amorphous polymers. PVDF is a semi-crystalline polymer, therefore contributing to the low transparency due to light deflection by crystals, the structure was also observed to be much smaller than the ones in PS and PVC, suggesting the presence of crystals structure.

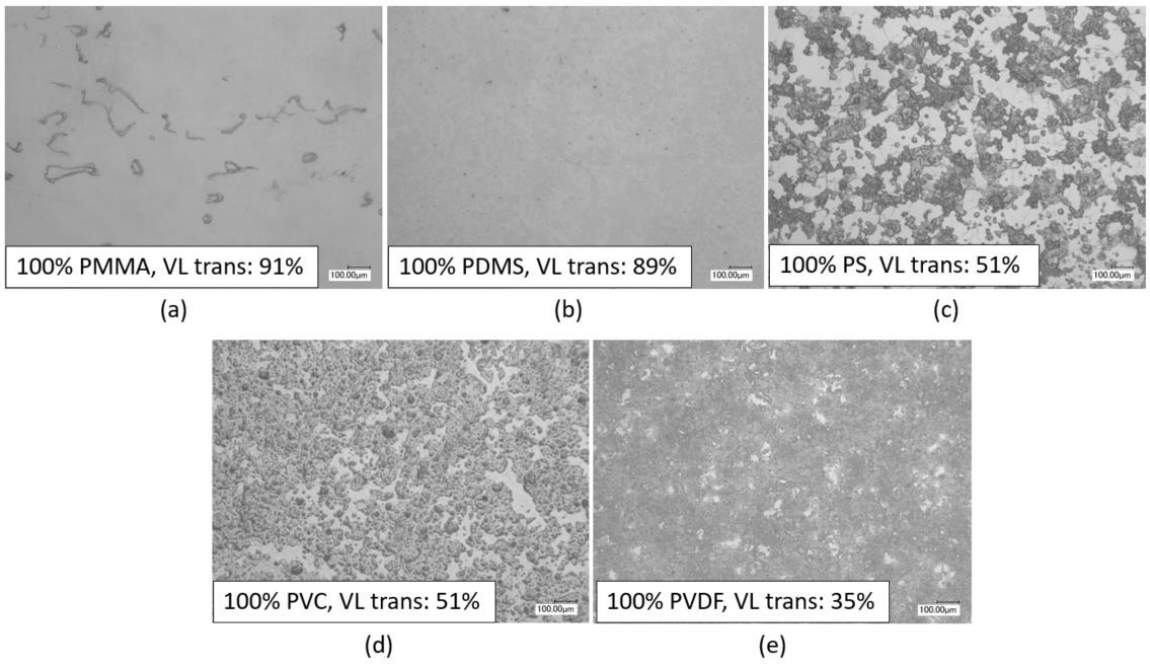

Figure 4.4. Microstructure of pure polymer coatings obtained at 200x magnification. (a) PMMA, (b) PDMS, (c) PS, (d) PVC, (e) PVDF.

4.2.2 Effect of blend formulation

PVC: For the same solution concentration, PVC is more viscous than PMMA, increasing the amount of PVC would promote aggregate formation as seen in 20/80

PMMA/PVC (Figure 4.5 (C)), similar to that of 100% PVC as discussed previously. Figure 4.5 (a) shows the structure of 80/20 PMMA/PVC, the coating was not as smooth as the one with 50/50 blending ratio, possibly because of uneven distribution of PMMA and PVC.

PS: The trend in structural changes for PMMA/PS coatings were similar to that of PMMA/PVC, the main difference is that PMMA and PVC are highly miscible, while PMMA and PS are immiscible. As such, bands of PMMA and PS are seen in 80/20 (Figure 4.6 (a)) and 50/50 (Figure 4.6 (b)) blends. Figure 4.6 (c) was obtained from 20/80 PMMA/PS and the structure was very similar to that of 100% PS, suggesting that PS became the dominant species within the blend.

PVDF: It was not possible for PVDF to reduce crystallinity just by dissolution and blending, therefore the amount of grains would directly reflect the amount of PVDF in the blends. The uniform orientations and distributions of grains suggests that the blending is homogeneous. At 80/20 ratio (Figure 4.7 (a)), amorphous regions of PMMA can be found and was still manage to produce a coating with high VL transmittance of 80%.

PDMS: The structure of PMMA/PDMS blends in Figure 4.8 remained relatively the same regardless of amount of PDMS. At 20/80 PMMA/PDMS (Figure 4.8 (c)), air bubbles have formed, possibly due to difficulty in dispersing PDMS evenly within the large amount of PMMA, where the viscosity values did not match well.

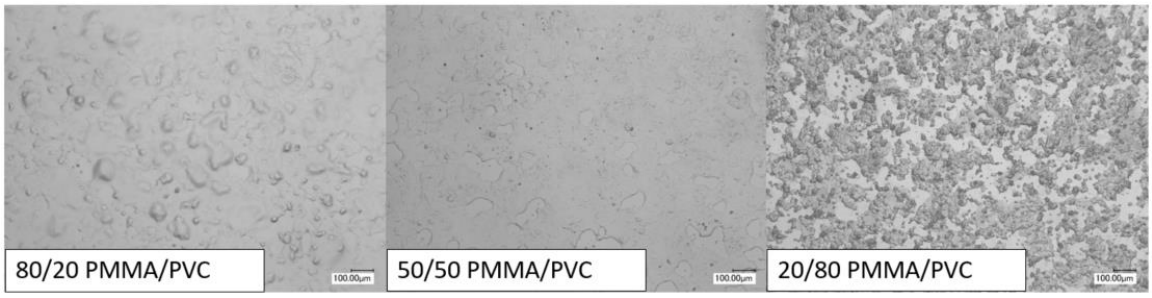

(a) (b) (c)

Figure 4.5. Structure of PMMA/PVC blends at (a) 80/20, (b) 50/50, and (c) 20/80 ratio.

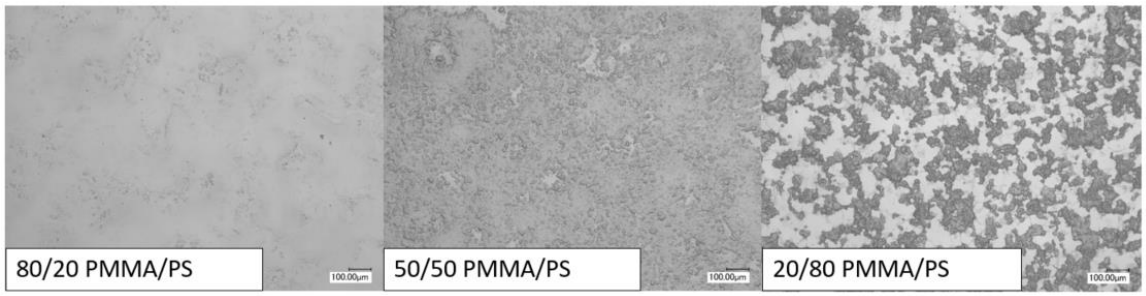

(a) (b) (c)

Figure 4.6. Structure of PMMA/PS blends at (a) 80/20, (b) 50/50, and (c) 20/80 ratio.

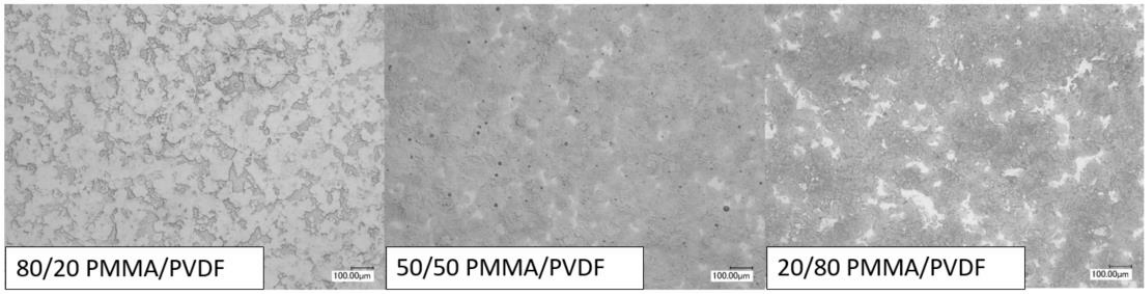

(a) (b) (c)

Figure 4.7. Structure of PMMA/PVDF blends at (a) 80/20, (b) 50/50, and (c) 20/80 ratio.

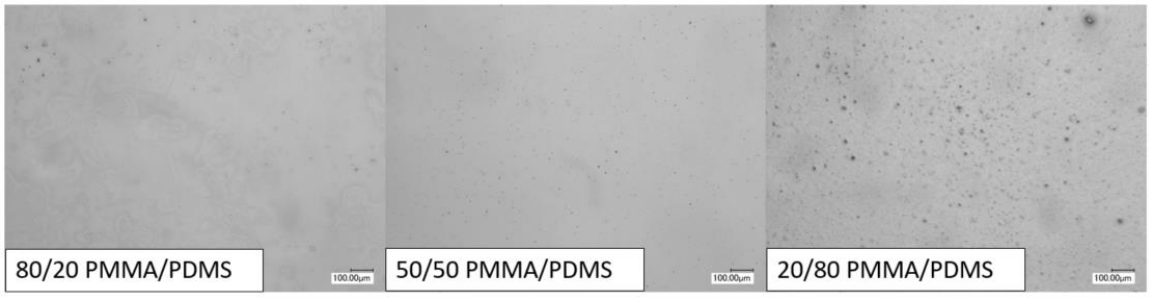

(a) (b) (c)

Figure 4.8. Structure of PMMA/PDMS blends at (a) 80/20, (b) 50/50, and (c) 20/80 ratio.

All secondary polymers individually have much higher capability to block UV and IR than PMMA, it is also observed that with the increasing amount of secondary polymer, roughness of surface also increased which allows higher reflection of solar radiation. This also explains why the addition of PDMS into PMMA had minimal effect on the improvement in solar heat gain as the coating surface remained smooth.

4.2.3 Effect of solvent

The appearances of the mixed solvent samples with 80/20 DMF:Acetone were white in color, the captured images showed high surface roughness with cloudy residues from the evaporation of acetone at the very top, which are evident in Figure 4.9 (a) PMMA, (c) PMMA/PS, (d) PMMA/PVC and (e) PMMA/PVDF. The surface smoothness of PMMA/PDMS in Figure 4.9 (b) was not affected by acetone as much, possible reason is that the low surface energy nature of PDMS allowed the fast dissipation of energy from acetone where condensation did not occur.

NeverWet shown in Figure 4.9 (f) was attached for reference purpose as it also contains acetone. The sprayed glass with NeverWet dried to a completely white layer, however cloudy residue was not found and the pores indicate that acetone left the surface completely. An explanation to the cloudy residue could be due to the impurities from the acetone and pre-treatment might be needed to reduce the whitening.

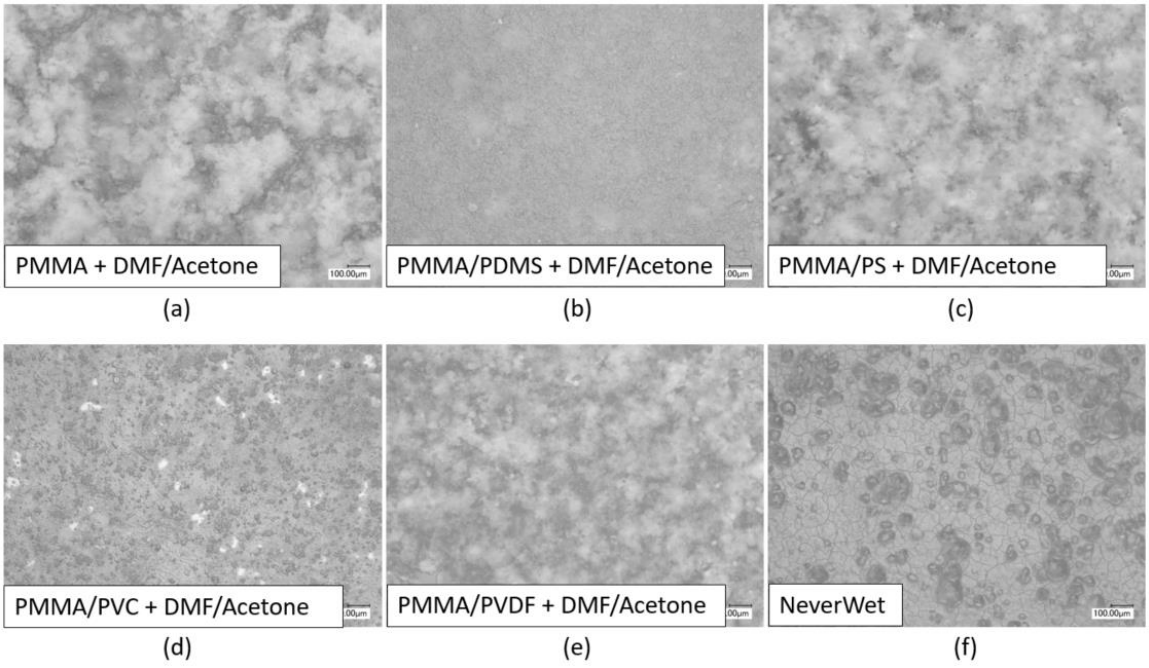

Figure 4.9. Structure of PMMA blends prepared from mixed solvent (a) – (e), and NeverWet coated glass (f).

4.3 Static Water Contact Angle

4.3.1 Effect of post-heat treatment

PMMA has been confirmed experimentally that it is hydrophilic with WCA of around 60^{o}, uncoated glass was measured to be 35^{o} as shown in Figure 4.10 (Left). The angles measured for the blends of PMMA/PVC, PMMA/PS, PMMA/PVDF, and PMMA/PDMS were 65^{o}, 72^{o}, 80^{o}, and 98^{o} respectively. As discussed in Chapter 3, the WCA of individual second polymers are higher than that of PMMA due to lower surface energy. By mixing them with PMMA, the WCA increased and the value lies in between that of PMMA and the second polymer. Proving that blending could be a low cost method

for improving wettability as opposed to physical and chemical modification of material or surface.

Figure 4.10 (Right) shows the measured WCA and the droplet morphology on post-heat treated surface. WCA was measured to be slightly higher except for PMMA/PS. The increase could be due to the increase in rigidity of surface roughness after curing, especially for PMMA/PVDF. Whereas for PMMA/PS the decrease was not significant and PMMA/PVC has stayed the same. For PMMA/PDMS, the increase was probably due to the evaporation of volatile substances, leaving behind only the low energy layer, which provides better hydrophobicity.

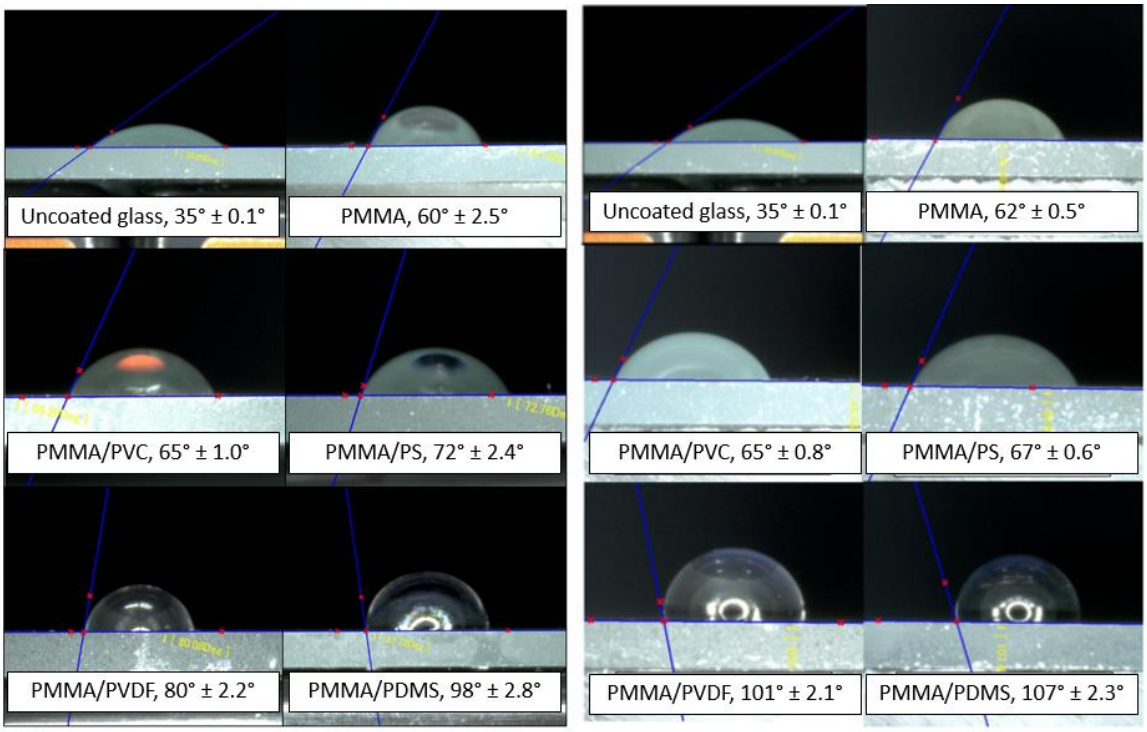

Figure 4.10. (Left) Without heat treatment, (Right) With heat treatment.

4.3.2 Effect of spray condition

The effects of spray distance and spray pressure on the change in water contact angle are graphed in Figure 4.11. The wettability of PMMA (black) was found to be non-sensitive to both parameters of spray distance and pressure, suggesting that pure polymers have higher tolerances to fabrication parameters than blended ones where the microstructure highly depends on the manufacturing procedure.

As the spray distance increased from 15 cm to 20 cm, the WCAs of the polymer blends decreased slightly in a linear fashion. When the spray distance increases, the as deposited layer is dryer, leading to possible porous film which structure cannot be altered much even with post-heat treatment at 40^{o}C, thereby losing the roughness rigidity to suspend the water droplet, and the droplet would tend to spread.

On the other hand, the WCAs peaked at 20 psi, and have decreased slightly for lower and higher pressure points. This can also be reasoned by the drying process which in turn affects the amount of roughness and stiffness of the film. Lower pressure has the same effect of higher distance, while higher pressure creates a wetter surface which could lose the necessary roughness for water repellency as the structure rearrange.

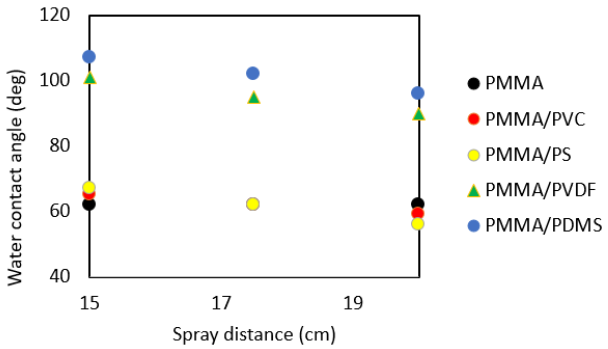

(a)

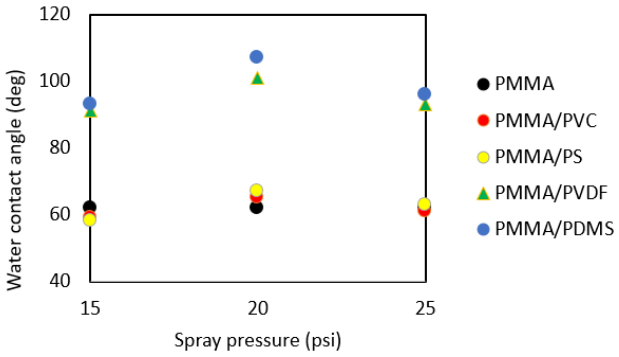

(b)

Figure 4.11. Effect of (a) spray distance, and (b) spray pressure on static WCA.

4.3.3 Effect of formulation

The effect of different ratio of PMMA within the blends on WCA was evaluated and recorded in Figure 4.12. In general, it follows the rule of mixture that the WCA reduces with increasing PMMA content. Each blend has reduced in a different extend, PDMS is the dominant contributor such that PMMA/PDMS stayed over 100^{o} for all combinations. PMMA/PVDF had a huge drop at 80/20 ratio, probably due to the uneven distribution of PVDF when the intermolecular forces during mixing were not favorable to disperse small amount of PVDF within PMMA; therefore, the wettability resemble that of PMMA more.

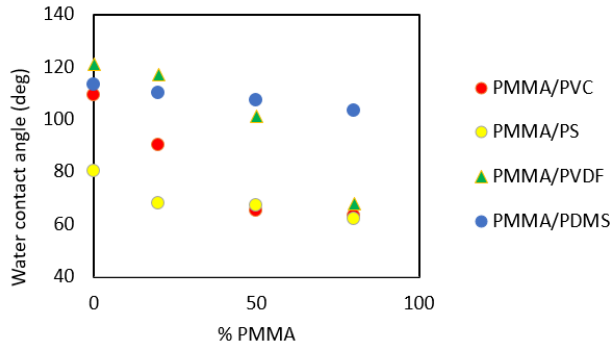

Figure 4.12. Effect of amount of PMMA in blends on static WCA.

4.3.4 Effect of solvent

An immediate jump of hydrophobicity was observed with the use of acetone, at 80/20 DMF/Acetone ratio, superhydrophobic state was almost achieved as shown in Figure 4.13, however, similar to the case of NeverWet, the self-cleaning effect was at the expense of transparency. Referring back to Section 4.2, the microstructure of the coatings prepared from DMF/Acetone was very rough, potentially having hierarchical structure which can contribute to suspending a water droplet. Table 4.8 shows the WCAs with and without acetone, the effect was most pronounced for PMMA/PVDF where the roughness could build onto the crystal structure.

Table 4.8. WCAs of PMMA and its 50/50 blends in DMF and DMF/Acetone systems.

Material	DMF	DMF/Acetone 80/20
PMMA	62° ± 0.5°	122° ± 1.3°
PMMA/PVC	65° ± 0.8°	82° ± 1.2°
PMMA/PS	67° ± 0.6°	120° ± 1.7°
PMMA/PVDF	101° ± 2.1°	147° ± 3.2°
PMMA/PDMS	107° ± 2.3°	133° ± 3.6°

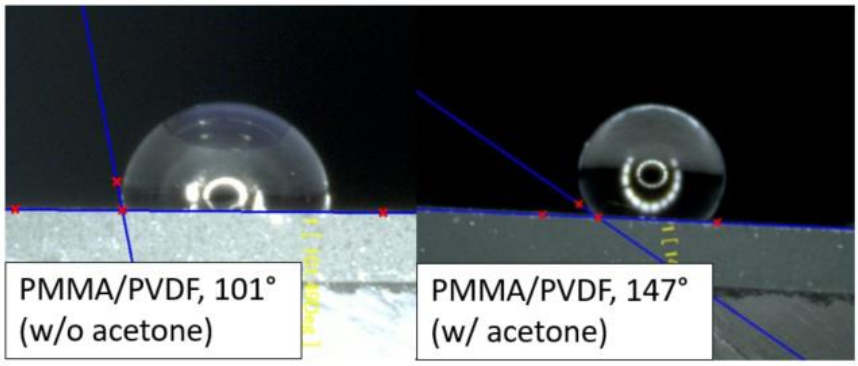

Figure 4.13. Improvement of water repellency for PMMA/PVDF.

4.3.5 Product comparison

The WCAs of RainX and the 3M insulator film were measured to be 95° and 85°, respectively. By comparing the WCA and transmittance data, it can be concluded that PMMA and its blends such as PMMA/PDMS could be used as an alternative material for window and windshield coating, as opposed to only using siloxane as primary binder. The addition of PMMA can offer better heat resistance during the hot days, and potentially reducing heat loss during the cold days as well, it also provides better durability and weather resistance as discussed in Chapter 2.

4.4 Dynamic Water Droplet Behavior

The dynamic behavior of water droplet for two sets of samples including the individual polymer coatings and the 50/50 blends have been studied for their on-set of departure and the rolling along the surface with respect to wind speed. Incline angles of 0° and 30° were studied, the 15-second averaged air speeds are recorded in Table 4.9.

Table 4.9. Averaged wind speeds for on-set of departure, rolling, and balancing gravitational force.

unit: km/hr	0°		30°	
Material	On-set of departure	Wind speed during roll off	Wind speed that balances Fg	Wind speed during roll up
PMMA	6.1	9.3	10.8	12.2
PVC	5.4	6.4	7.5	9.3
PS	6.4	8.2	8.2	12.9
PVDF	8.6	11.5	11.5	14.7
PDMS	4.3	6.1	6.8	7.5
PMMA/PVC	5.9	7.9	10	12.9
PMMA/PS	6.1	8.6	9.7	14.7
PMMA/PVDF	7.5	9	10	13.3
PMMA/PDMS	5.7	8.2	8.6	14
RainX	4.3	5.7	6.4	7.9

4.4.1 On-set of departure for 0^o incline

The on-set of departure was defined as when droplet started to move slowly on the coated surface, the aerodynamic forces caused the droplet to deform and ready to move. For reference, at 0^o incline, droplet on RainX started to move at 4.3 km/hr. Among the investigated pure polymer coatings, PDMS was the most slippery where its performance matched that of RainX. PVC was measured to be more slippery than PMMA and PS. The observation could be attributed to the surface energy of polymers, for which PDMS was the lowest, and PVC has lower surface energy than PMMA. The surface of PVC was homogeneous as shown from microstructure whereas structure of PS was found to be larger with aggregates. PVDF is crystalline leading to rough surface, although it has low surface energy, it was found that a rough surface might induce more contact area and interlock with the water droplet than a smooth surface like PDMS and PMMA.

The on-set of departure for coatings made of 50/50 polymers blends showed same trend as the pure polymers, but at a higher value, due to increase in overall surface energy induced by PMMA. According to the microscope images, PMMA/PDMS was flat, smooth and completely amorphous; together with lower surface energy, it allowed easier departure of water droplet. PMMA/PVC is homogeneous in terms of mixing, the structure was small, therefore the interlocking with water droplet was not as much as PMMA/PS. PMMA/PS has banded structure of PMMA- and PS-rich regions, the air speed that caused the on-set of departure was lowered as compared to 100% PS, but resembling more of PMMA, possible reason is that PMMA filled up the gap between PS aggregates and reduce the roughness. The on-set speed for the blends remained the highest for PMMA/PVDF, the speed was also found to be lower than pure PVDF alone; the same might apply to

PMMA/PVDF where PMMA has filled the space between crystals. In general, the on-set lied between that of PMMA and the second polymer when they were blended, following the rule of mixture.

4.4.2 Translation of water droplet for 0^o incline

In order to set the droplet to translate across the coated surface, a higher air speed was required, and was calculated to be on average an increase of 34% as compared to the on-set of departure. The moving of droplet was observed to be primarily a shift of volume which became the driving force for acceleration of droplet. The shifting of volume was different depending on the coating material, which was related to the interaction between the droplet and the surface. More slippery surfaces would have less shifting of volume which can be evaluated by the increase in droplet height; where more contact between droplet and surface would cause higher resistance to movement.

RainX showed the fastest droplet movement which moved for the same amount of distance within a shorter period of time, followed by PDMS, PS, PVC, and PMMA. Besides the relationship between the dynamic behavior with microstructure and surface energy, the interactions between the droplet and surface could also be explained from the electrostatic point of view. Organic molecules are generally neutral in charge states, the electrons are delocalized entities within their orbitals, which can induce polarity effects.

The substituents of the molecules are classified into electron donating and with-drawing groups, the nature of electrostatic forces state that opposite charges are attracted to each other, while same charges would repel. The substituent groups in the polymers used include the chloride (Cl) in PVC, fluoride (F) in PVDF, phenyl (C_6H_6) in PS, ester

($OOCH_3$) in PMMA, and methyl (CH_3) in PDMS. Water molecule is slightly electron donating from the oxygen, therefore the polymers containing electron donating groups such as PDMS and PS, the surfaces repel each other during the translation leading to higher velocity of water droplet. Whereas PMMA, PVC and PVDF contain electron withdrawing groups, increasing the interactions with water molecules, leading to longer contact and more constant velocity during the translation across the coated surfaces.

The shots for the translations are presented below for each coating:

RainX: Shape of droplet maintained well, the deformation was minimal and droplet accelerated, as seen at 0.75 seconds in Figure 4.14.

PMMA: The height of droplet increased, the volume shifted from left to right which drove the movement; the bottom of droplet attached to the surface as seen in Figure 4.15.

PVC: The droplet was observed to wobble, droplet edges lifted, and the air pushed the droplet such that it landed on the right which induced the movement, as seen in Figure 4.16.

PS: The droplet initially refused to deform until 1.5 seconds, which then caused an acceleration of droplet as the weight being pushed downward, as seen from Figure 4.17.

PVDF: Deformation of droplet was found to be the largest, the height of droplet rose and the shape became triangular. Wore contact with the surface was induced by the droplet elongation, shape was not maintained during the movement, as seen in Figure 4.18.

PDMS: The droplet shape maintained well during the translation, the height of droplet remained similar, shifting of weight from left and right was evident, as seen in Figure 4.19.

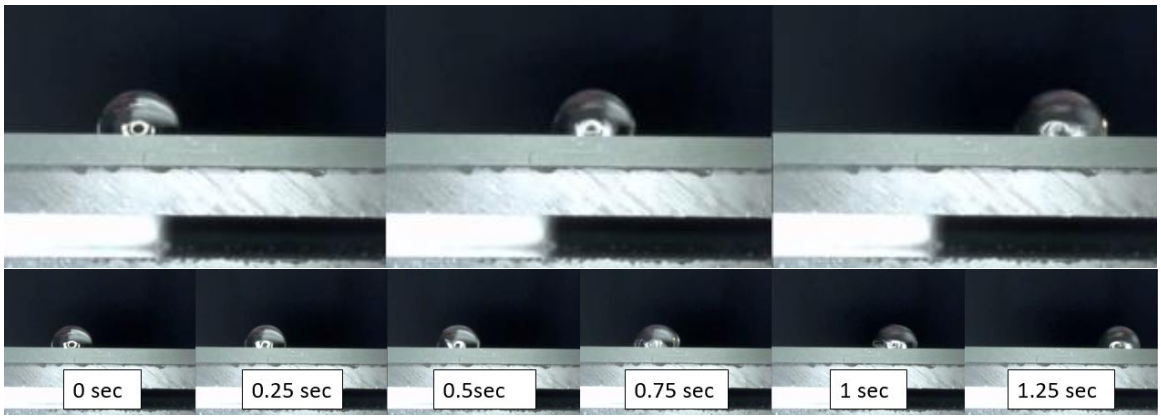

Figure 4.14. Deformation and translation of water droplet on RainX coated surface.

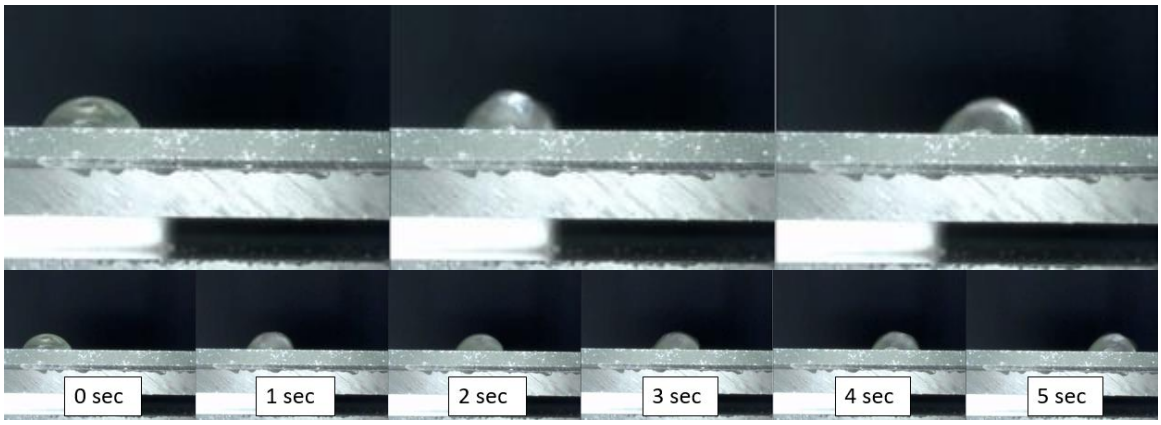

Figure 4.15. Deformation and translation of water droplet on PMMA coated surface.

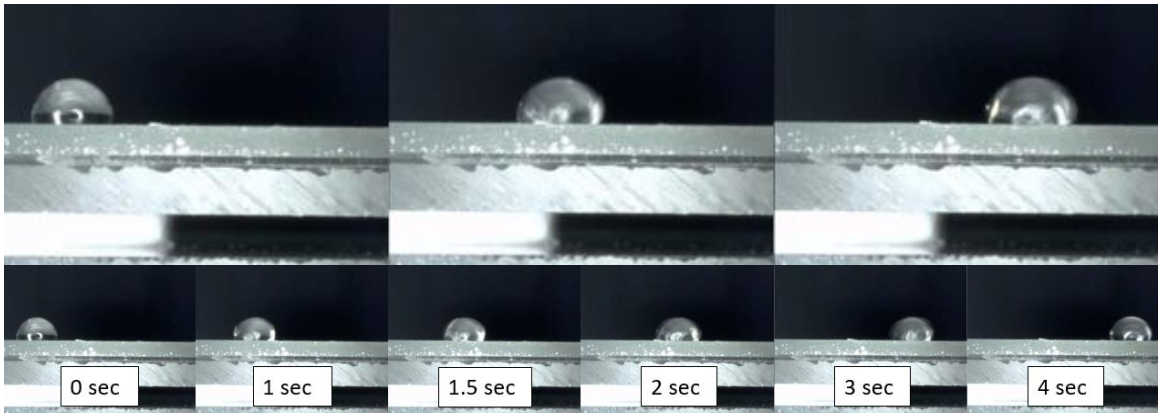

Figure 4.16. Deformation and translation of water droplet on PVC coated surface.

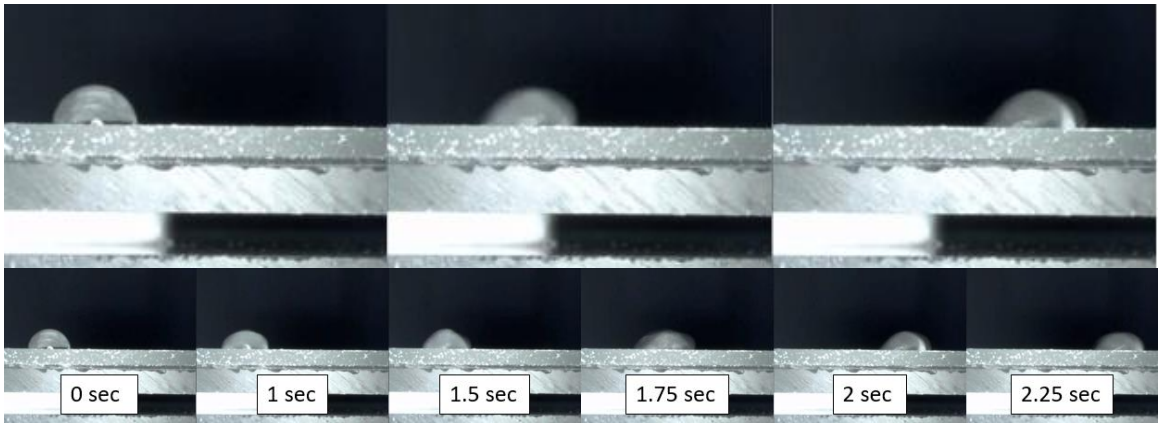

Figure 4.17. Deformation and translation of water droplet on PS coated surface.

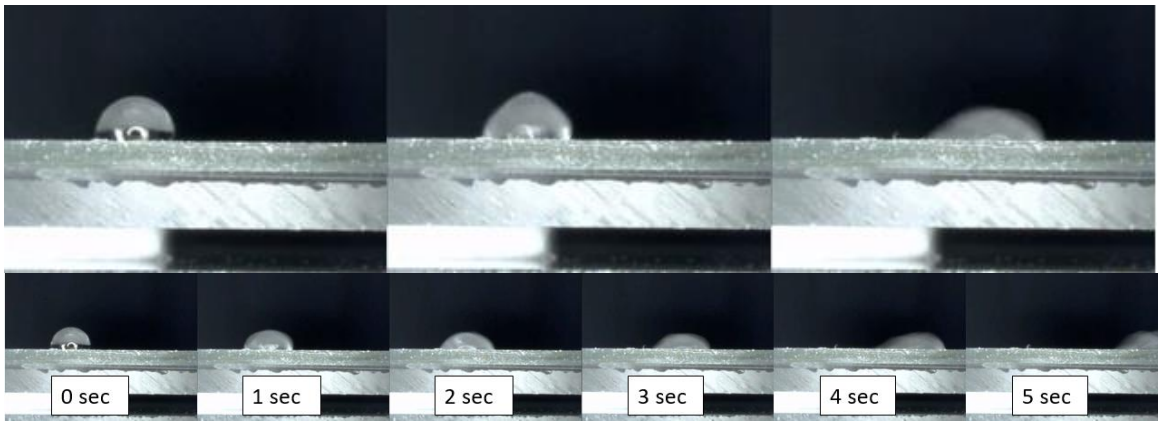

Figure 4.18. Deformation and translation of water droplet on PVDF coated surface.

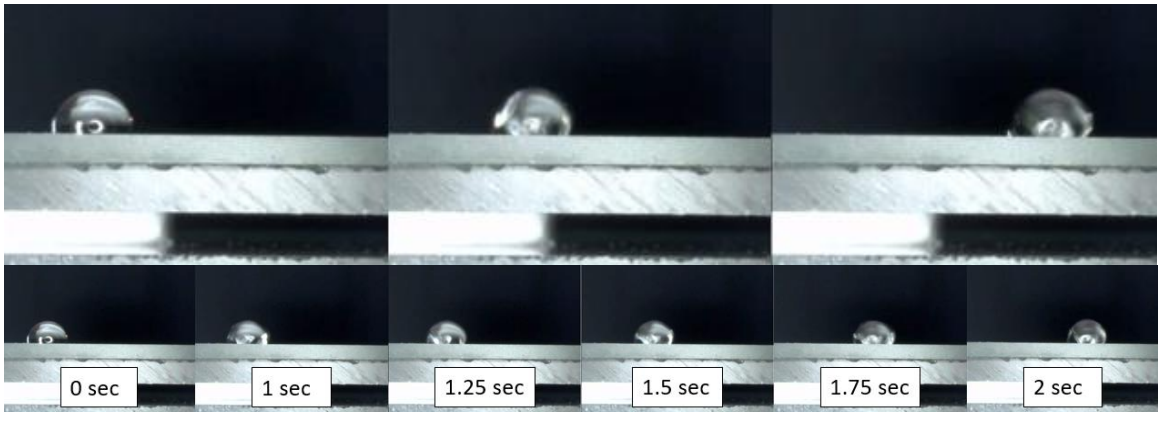

Figure 4.19. Deformation and translation of water droplet on PDMS coated surface.

The blending of pure polymers with PMMA led to increase in the required air speed to set the water droplet off to roll across the coated surfaces, except for PMMA/PVDF. The shots for the translations are presented in Appendix B.

PMMA/PVC: The air speed increased by 24%, primarily due to higher overall surface energy. The WCA for the blend was measured to be lower than pure PVC coated surface, the droplet mainly deformed at the top of the droplet where the contact length remained similar throughout the translation.

PMMA/PS: The air speed was measured to be similar, the mixing of PMMA and PS neutralized the charges as PMMA is electron withdrawing and PS is electron donating, this neutralization is likely to compensate for the increase in surface energy. The droplet moved by wobbling and vibration and took less time to translate than PMMA/PVC.

PMMA/PVDF: The blending has reduced surface roughness by filling the gaps between PVDF crystals with PMMA. Although the air speed requirement reduced as compared to pure PVDF coating, it still remained the highest among the blends. The droplet resisted to move initially, the shape of droplet changed from round to triangular, it then shook in all directions to translate across the coated surface.

PMMA/PDMS: The air speed increased by 34% as it had the largest increase in overall surface energy. There was little vibration during the translation, there was evident of droplet acceleration by the change in hysteresis, as such, the shape did not maintain as well compared to PDMS surface.

Angle of hysteresis including the advancing and receding angles were measured during translation on 0^o incline, 10 measurements were taken at half way of the translation, the averaged angles were compared with the static WCA and are presented in Table 4.10. For PMMA surface, the droplet had slight increase in advancing and reduce in receding angles by 6.5% and 13%, respectively.

Water droplet on PVC and PS coated surfaces tend to deform in the height direction where the volume was shifted from receding edge with a decrease in angle, and the advancing angle had no change from static WCA. The elongation of droplet during the translation caused the angles of hysteresis to be small as compared to the static WCA for PVDF surface. Angles of hysteresis both decreased for PDMS, possibly due to a slippery surface where deformation of droplet happened on both the top and bottom of the droplet. It can be concluded that higher static WCA does not necessarily result in more slippery surface.

For the blends of polymers coated surfaces, the mixing with PMMA resulted in the addition of characteristics from PMMA. PMMA/PVC and PMMA/PS had an increase in advancing angle and decrease in receding angle for less than 20%. PMMA/PVDF had lower static WCA than PVDF, there was large resistance to droplet movement which was evident by the same static WCA and advancing angle, as well as the 45% reduction for receding angle where the tail lagged behind. All angles for PMMA/PDMS are similar, suggesting that the shape of water droplet maintained well during the translation, and behaved similar to market product RainX.

Table 4.10. Averaged angle of hysteresis comparison with static water contact angle.

Material	Static WCA (deg)	Advancing (deg)	Receding (deg)
PMMA	62	66	54
PVC	109	108	91
PS	80	78	53
PVDF	121	80	37
PDMS	113	101	97
PMMA/PVC	65	77	59
PMMA/PS	67	70	53
PMMA/PVDF	101	102	56
PMMA/PDMS	107	98	92
RainX	95	104	92

4.4.3 Force balancing of droplet for 30^{o} incline

The balancing of droplet from gravitational force was considered when the advancing angle equaled receding angle. Droplet had the tendency to slide down slowly on slippery surfaces such as PDMS, PVC, in turn, the droplet was also easy to be pushed up the incline of 30^{o}. The air speed required to balance the force for PDMS was similar to RainX due to their low surface energy of siloxanes; while PVC was observed to be slippery due to the surface also being relatively hydrophobic and PVC is amorphous with low surface roughness. The aggregates of PS and the high surface energy prevented the water droplet from deforming due to gravity, therefore the air speed requirement was lower than that of PMMA, which has higher surface energy than PS although it is smoother. PVDF required the highest air speed to balance off gravity among the pure polymer coated surfaces, with the largest static WCA measured with the least amount of contact in the

width direction, the weight of the advancing side was therefore the largest and required the most force to balance.

After blending the polymers with PMMA, it caused 50% increase for the force needed to balance for PMMA/PDMS due to the increase in overall surface energy to overcome. The speed measured for PMMA/PVC, PMMA/PS, and PMMA/PVDF were the same at about 10 km/hr, which was an increase for PMMA/PVC and PMMA/PS as expected from the increase in surface energy and the similar static WCA measured for the two. However PMMA/PVDF was a decrease in required force compared to pure PVDF, probably due to reduction in surface roughness and static WCA where weight is better distributed along the contacted region.

4.4.4 Translation of water droplet for 30^{o} incline

The 30^{o} incline was a simulation of a moving vehicle where water droplets roll up the windshield during forward drives. 30^{o} was chosen for the study as it is the typical angle for many car models. In order to set the water droplet rolling up the incline, the force in the traverse direction that is parallel to the incline needs to be greater than the gravitational force and the surface tension. The measured air speed required to cause the droplet to roll up was determined to be on average 34% higher than the speed required to balance gravity.

PDMS required the lowest air speed similar to that of RainX, the deformation of water droplet during translation were also similar as seen in Figure 4.20 and Figure 4.25, except PDMS could maintain hydrophobicity better with higher receding angle. PVC was second to PDMS with slight increase in air speed while it also maintained hydrophobic

state throughout the translation as shown in Figure 4.22. The shapes of droplets on PMMA surface in Figure 4.21 and PVDF surface in Figure 4.24 showed the same trend in moving mechanism, where the height of droplet increased and weight of droplet was shifted from top to right to drive the translation. Air speed required for droplet on PS surface was similar to that of PMMA, the droplet refused to move at first due to the surface roughness.

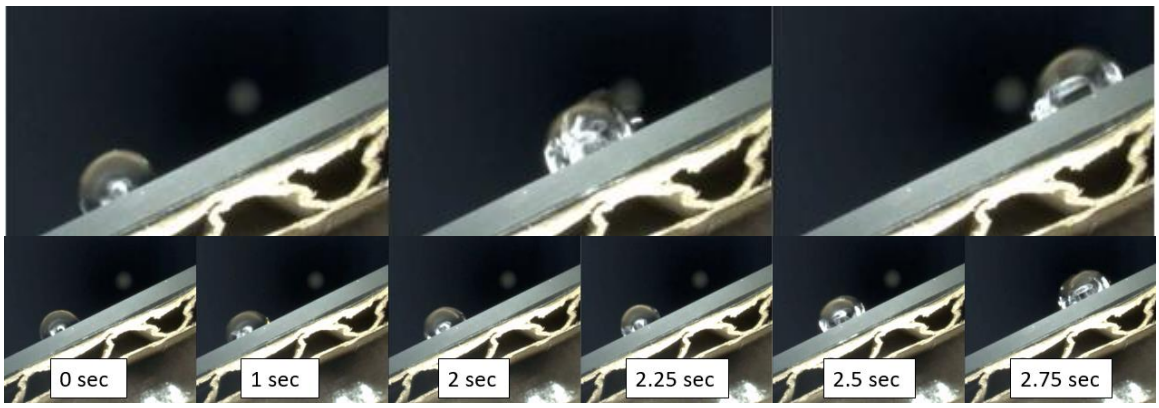

Figure 4.20. Translation of water droplet on RainX coated surface at 30^{o} incline.

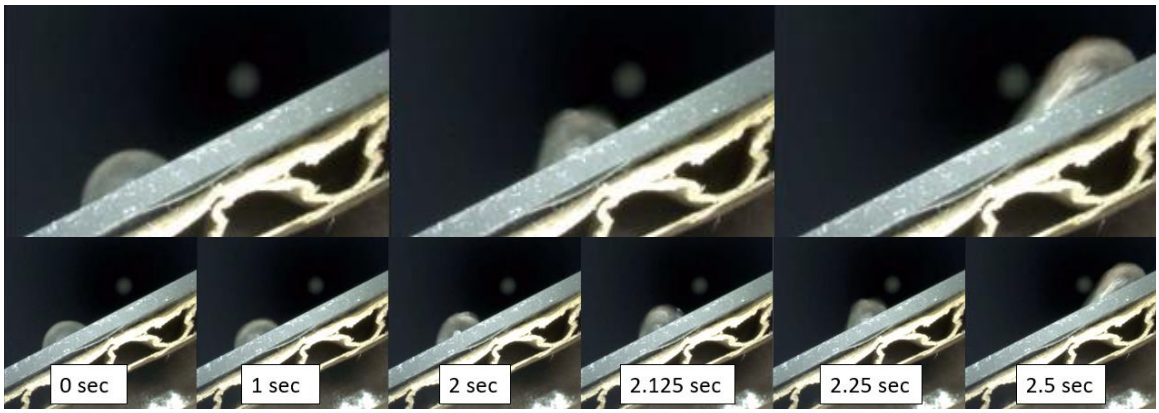

Figure 4.21. Translation of water droplet on PMMA coated surface at 30^{o} incline.

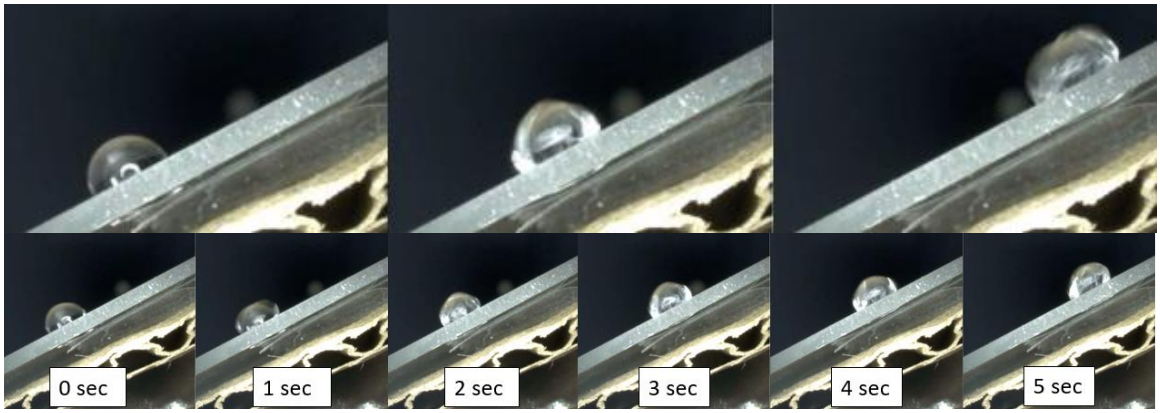

Figure 4.22. Translation of water droplet on PVC coated surface at 30^{o} incline.

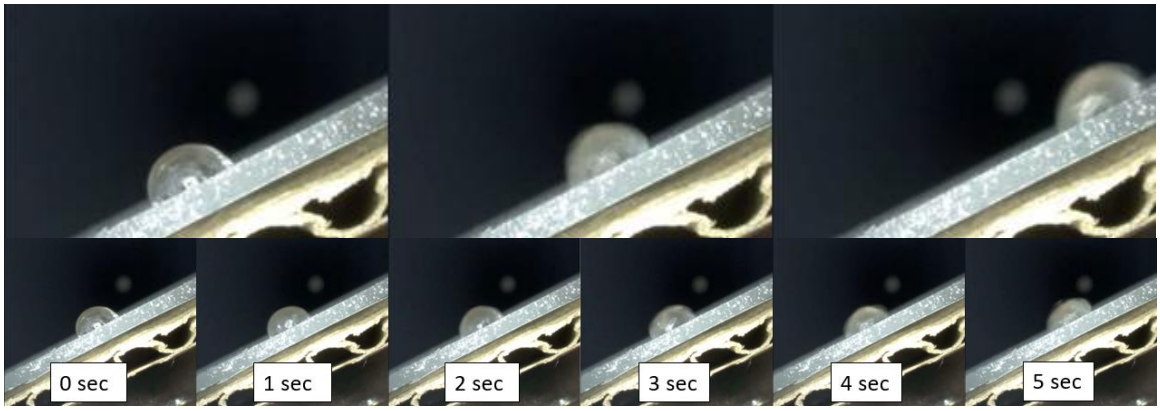

Figure 4.23. Translation of water droplet on PS coated surface at 30^{o} incline.

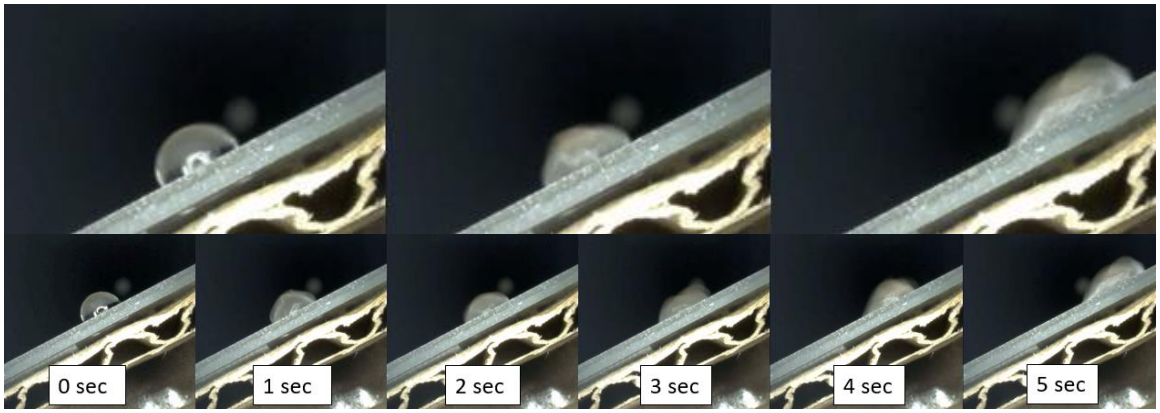

Figure 4.24. Translation of water droplet on PVDF coated surface at 30^{o} incline.

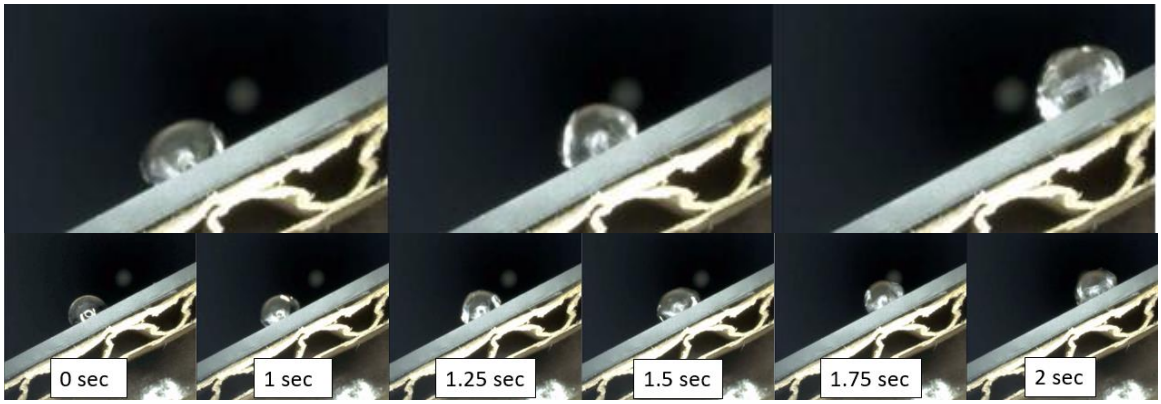

Figure 4.25. Translation of water droplet on PDMS coated surface at 30^{o} incline.

The schematics for the water droplet deformation and translation for the polymer blends coated surfaces are presented in Appendix B2. The recorded air speeds for driving the droplet to roll upward on 30^{o} incline were found to be almost the same for all blends with PMMA at around 13 and 14 km/hr. With the addition of PMMA, the droplet resisted movement at moderate air speeds of about 10 km/hr, wobbling of droplet was not enough to lift the edges of the droplet to promote translation. On average, it required an increase in speed by 2.4 km/hr for the blends than pure polymer coated surfaces.

It should be noted that the velocity presented in Table 13 is a relative value with respect to the droplet size of 2.5 mm in diameter. The average raindrop size before hitting an object near ground level is determined to be 5 mm in diameter. A scaling factor is needed to determine the actual velocity of the droplet in reality using the similarity requirements as shown in Equation 9, where V, d, and denote air velocity, diameter of droplet, and dynamic viscosity, respectively. The environments for both experimental and actual raining condition are the same where air is the only gas present, therefore the dynamic viscosity terms are cancelled. If the experimental droplet is half the size of the raindrop,

then $d_{exp} = ½\ d_{rain}$, in order to balance the equation, V_{rain} will therefore be 2 times the speed of V_{exp}.

$$\left(\frac{V d}{\upsilon}\right)_{exp} = \left(\frac{V d}{\upsilon}\right)_{rain} \qquad (9)$$

Chapter 5. Conclusions and Recommendations for Future Work

Nowadays, there is a strong interest in finding solutions to help decrease our environmental footprint as well as to decrease accident hazards in our daily lives. Unprotected external glass surfaces on buildings and automobiles present two major issues: they allow high transmittance of light waves causing noticeable thermal gradients between indoors and outdoors which promote the increase usage of heating and air-conditioning usage throughout the year. On the other hand, vehicle glass surface wetting during precipitation can reduce visibility, raising safety concerns. This research has addressed these two major issues with a single solution. An affordable polymer-based hydrophobic coating for glass surfaces was proposed and studied to solve the two problems at the same time.

The coatings were made of poly(methyl methacrylate) (PMMA) and its blends with poly(vinyl chloride) (PVC), polystyrene (PS), poly(vinylidene difluoride) (PVDF), and poly(dimethyl siloxane) (PDMS). The coatings were designed and developed on glass substrates through the method of spray deposition with compressed air and a conventional dual trigger air brush. All formulations were successfully developed and deposited from dissolved state. The final transparent products adhered well without signs of peeling and homogeneous structures were achieved for the blended coatings.

Characterizations on the transmittance, microstructure, wettability, and the dynamic droplet behavior were performed to evaluate the performances of the developed coatings. The relationships between the coating performances of wettability, dynamic droplet behavior under influence of air flow, and transmittance with intrinsic material

properties of crystallinity, organic substituent, and surface energy were presented. The following are the conclusions made from the experimental observations and analysis:

- The post-heat treatment of coated glass at 40^{o} helped obtain uniform solvent evaporation and also enhanced transparency. The coatings were also found to adhere better to the glass surface than those coatings obtained via drying in air with the same sprayed material and procedure.
- PMMA provided excellent transparency and adhesion on glass substrate, and blending of PMMA with the other polymers offered many opportunities to tailor the desired properties for the target applications. The secondary polymer can provide protection from thermal radiation, and can improve water repellency.
- It was found that there were no significant changes in transmittance and static water contact angle due to the spray conditions of distance and pressure. The base referencing parameters of 15 cm and 20 psi at 5 wt% concentration were found to be optimal for most polymeric materials.
- The use of acetone in the solution system provided faster solvent evaporation and lead to higher surface roughness resulting in water contact angle close to superhydrophobic state.
- Some of the fabricated coatings in this work were comparable or superior to some products currently available in the market that address either hydrophobicity or offer protection towards solar radiation. For example, the blend of PMMA/PDMS was observed to have the same visible light transmittance but more hydrophobic than the commercially available water repellent spray by RainX. The PMMA/PDMS coating from this work showed that it could block 18% more of infrared to lower the solar heat

gain. The blend of PMMA/PVDF could block 17% more heat than RainX and offered even higher protection from both ultraviolet and infrared radiations than a commercially available insulator film by 3M, while maintaining reasonable visible light transmittance of 72%. PMMA/PVC, on the other hand, was not hydrophobic, the surface was found to be slippery and showed amorphous and homogeneous structures. This caused the droplet to roll away from PMMA/PVC coated surface at similar wind speed measured as the surface coated with PMMA/PDMS. The blend of PMMA/PVC also offered moderate radiation shielding, which can also be a possible alternative.

- This work demonstrated the viability of optimizing the final properties by altering the formulations. For example, surface roughness was observed to increase with decreasing PMMA content, whereas wettability decreases with higher PMMA content.
- The dynamic analysis carried out in this research presents a novel characterization in the field. Many have only performed characterizations on droplet bouncing, dropping, and roll-off analysis; whereas the translation of water droplets with time and air flow speed at 0^o and 30^o incline in this work can provide insight in coating development for moving objects such as a vehicle.
- The deformation of water droplets due to the blowing of air was recorded and the translation mechanism was able to be observed clearly. Higher vibration and wobbling of the droplets were seen for less hydrophobic and less slippery surfaces as the droplets resisted to move. Whereas for slippery surfaces, the shape of the droplets was maintained to a high degree and the hydrophobicity of the surfaces was well retained at the receding edge. Overall, weight shifting was the dominant cause of movement.

Comparative study was performed for the effect of post-heat treating for curing, varying spray conditions of spray pressure and spray distance, different volume ratios of polymer contents in the blends, and the presence of mixed secondary solvent. Overall, the developed coatings showed promising results which suggest their great potential for the applications for glass surfaces to passively regulate indoor climate by altering the radiation transmittance, which is believed to lower the environmental impact if heating and cooling usage can be reduced. The hydrophobicity observed in the coatings can prevent wetting of the glass surfaces, which then improves visibility and safety of vehicles. To improve on the performances of the developed coatings in this research, the following future work is recommended:

- This study only included binary blending systems, where PMMA was selected to be the primary polymer of blends. The blending of PVC, PS, PVDF, and PDMS without PMMA can be studied. Tertiary blending systems should also be explored.
- The secondary solvent, acetone, used in this study was difficult to control for its evaporation rate and is not ideal for applications where transparency is required. Other organic solvents can be considered, study on mixed solvent effect with various types of solvents introduced in Chapter 2.1.2 is worth investigating. The mixing of solvents can potentially alter the surface energy and microstructure of the coatings, resulting in a variety range of wettability and transmittance.
- Only polymers have been considered in this research, which served as the baseline study for coating development where formulations and various spraying parameters have been investigated. To incorporate more functions of the coatings besides thermal radiation shielding and water repellency, different classes of materials can be

considered to be included as dopants. This research serves as a base for smart coating development where the coatings could show intelligent reversible responses such as color changing, adjustable wetting behavior, and varying conductivity.

Appendices

Appendix A.

A1. TGA graphs of solvent evaporation rates

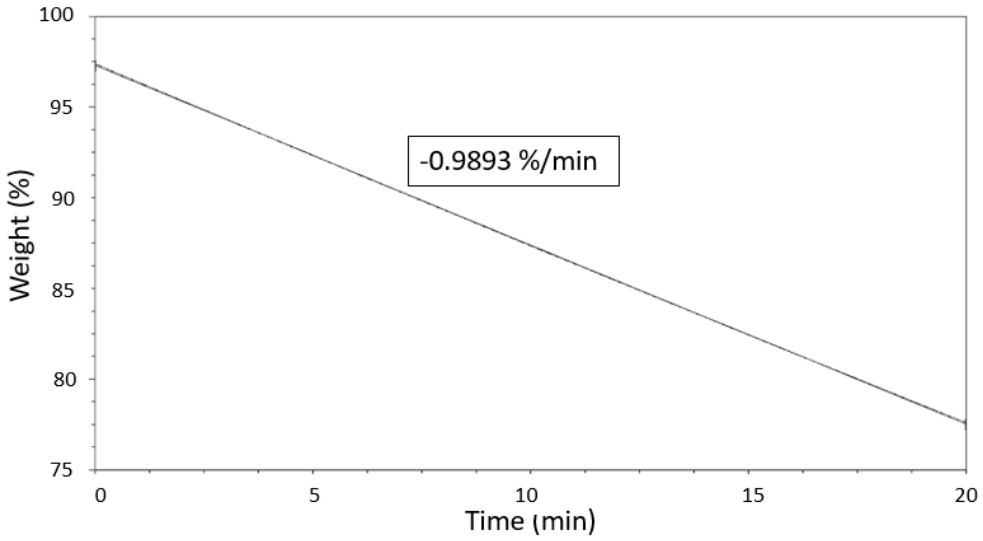

Figure A1. Evaporation rate of DMF.

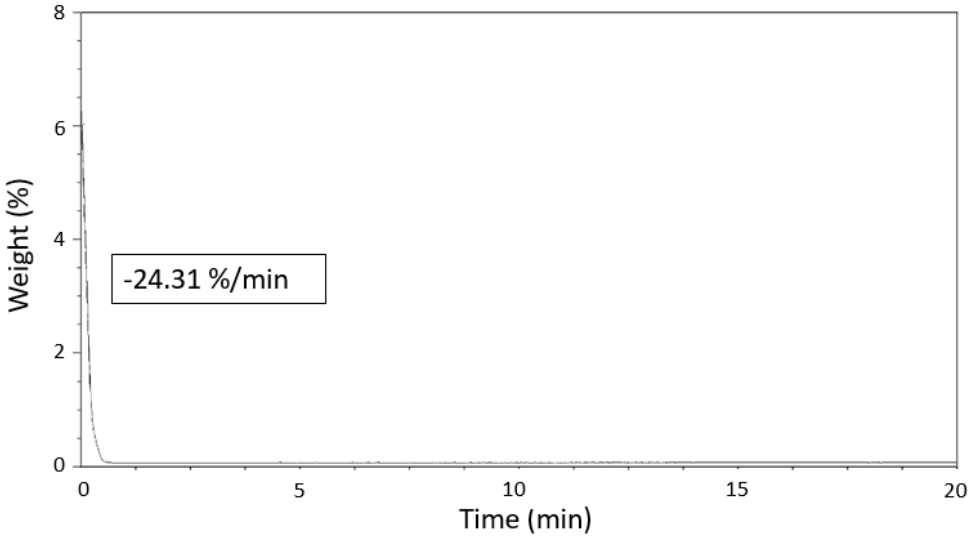

Figure A2. Evaporation rate of acetone.

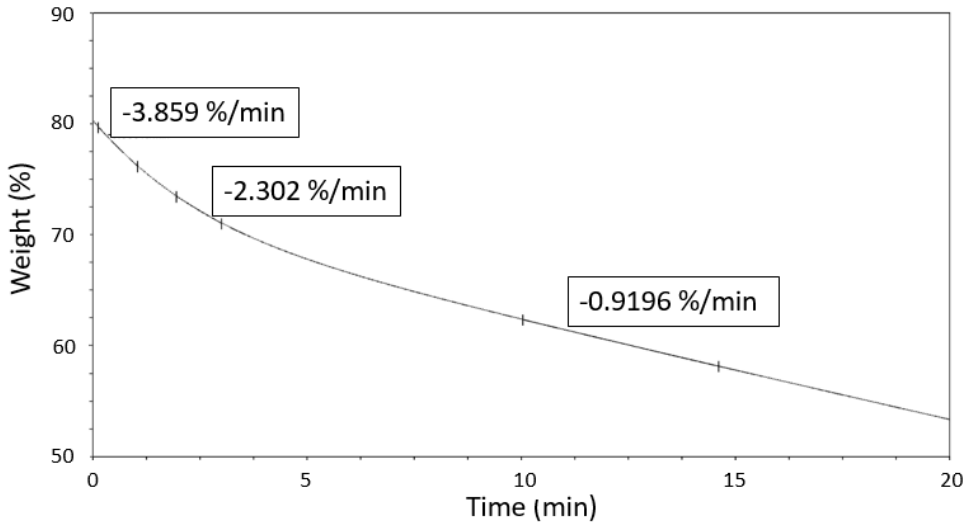

Figure A3. Evaporation rate of 50/50 DMF/Acetone.

Appendix B.

B1. Translation of water droplet on PMMA blends coated surface at 0^{o} incline

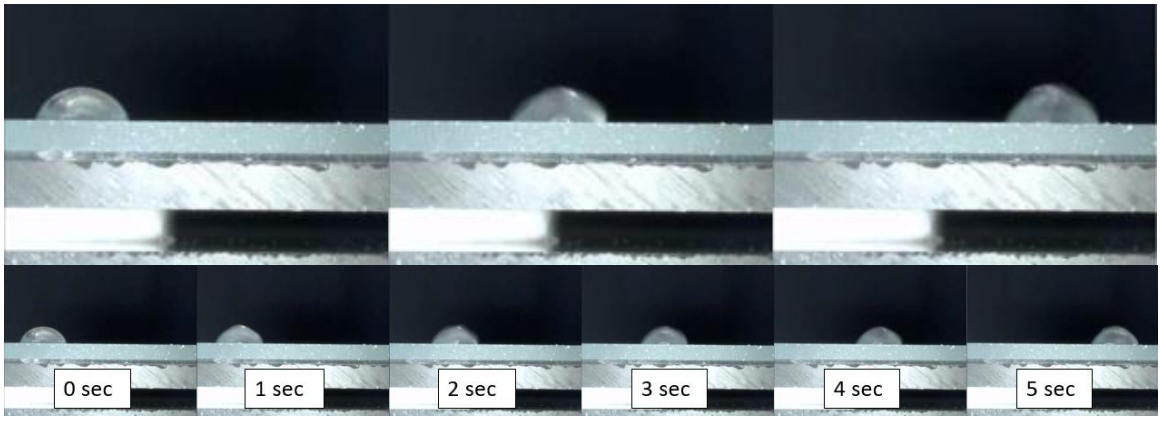

Figure B1. PMMA/PVC

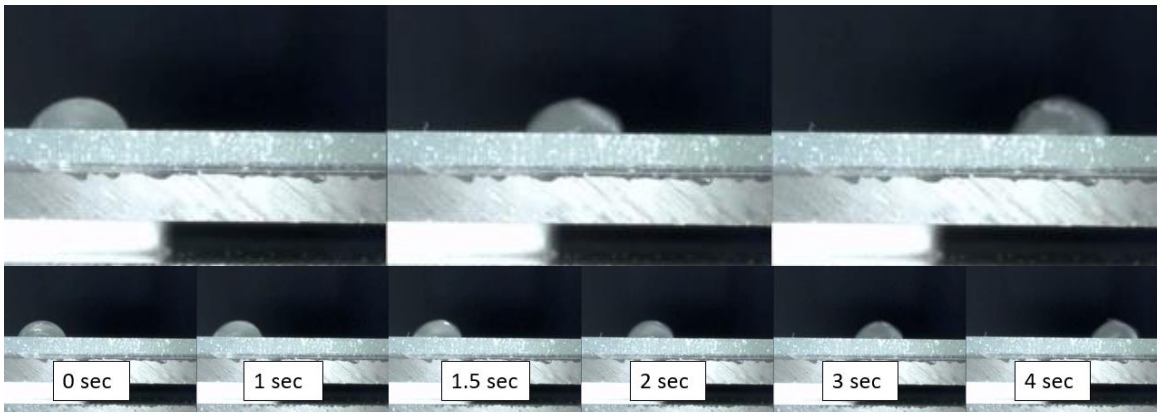

Figure B2. PMMA/PS

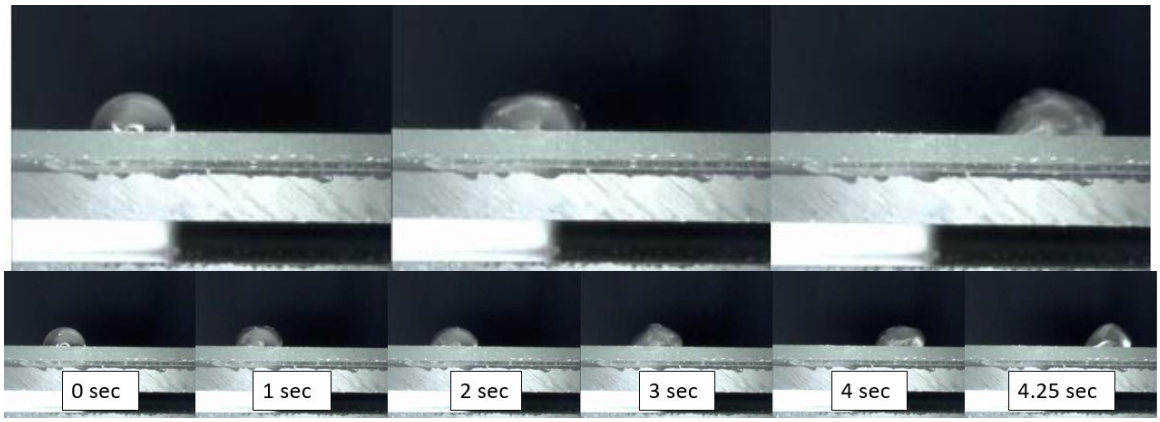

Figure B3. PMMA/PS

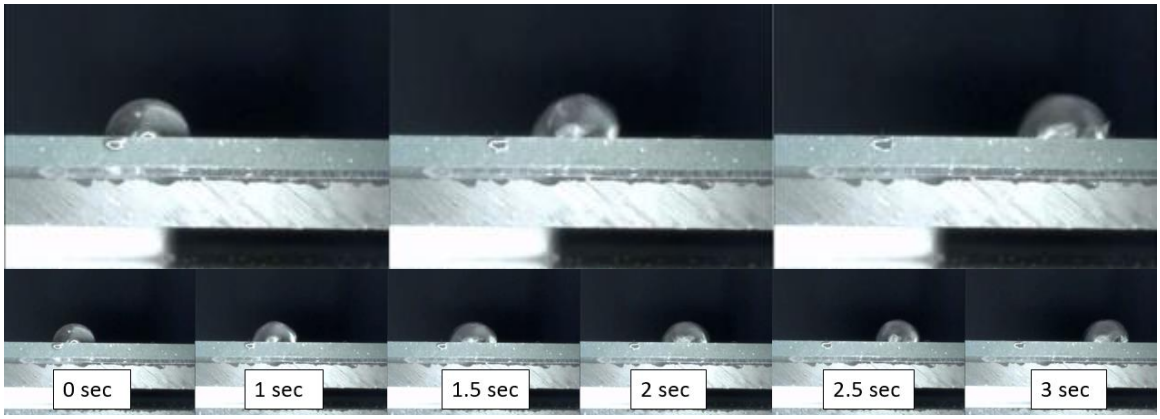

Figure B4. PMMA/PDMS

B2. Translation of water droplet on PMMA blends coated surface at 30^{o} incline

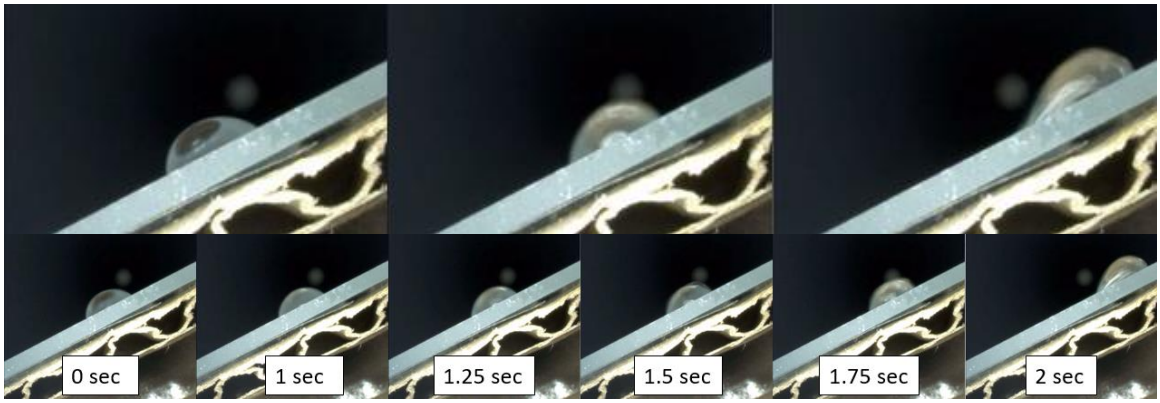

Figure B5. PMMA/PVC

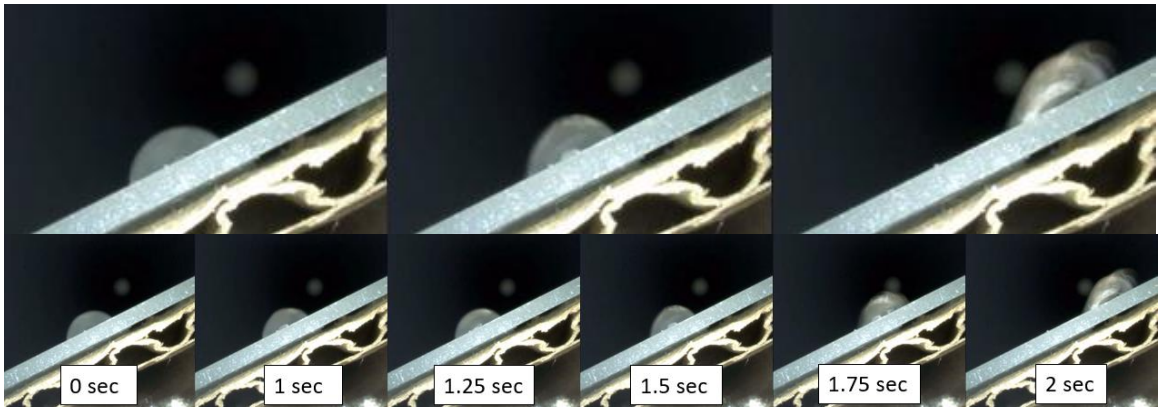

Figure B6. PMMA/PS

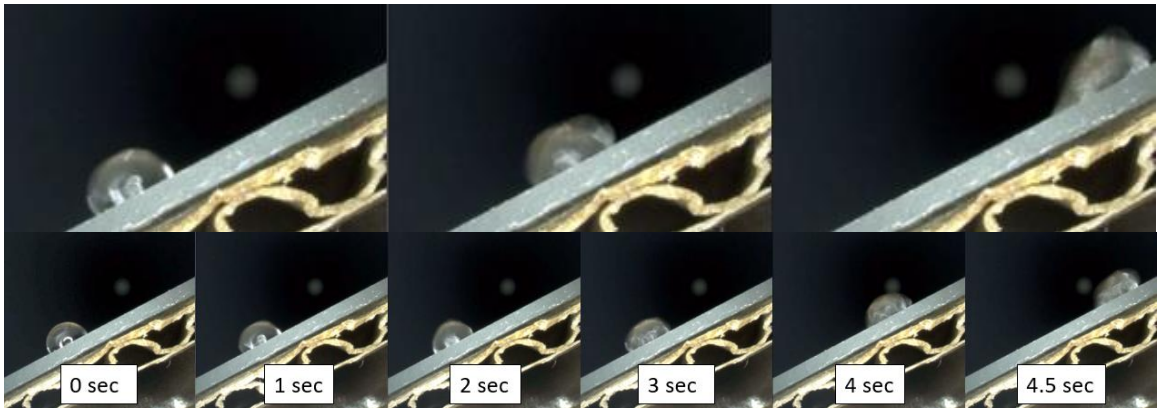

Figure B7. PMMA/PVDF

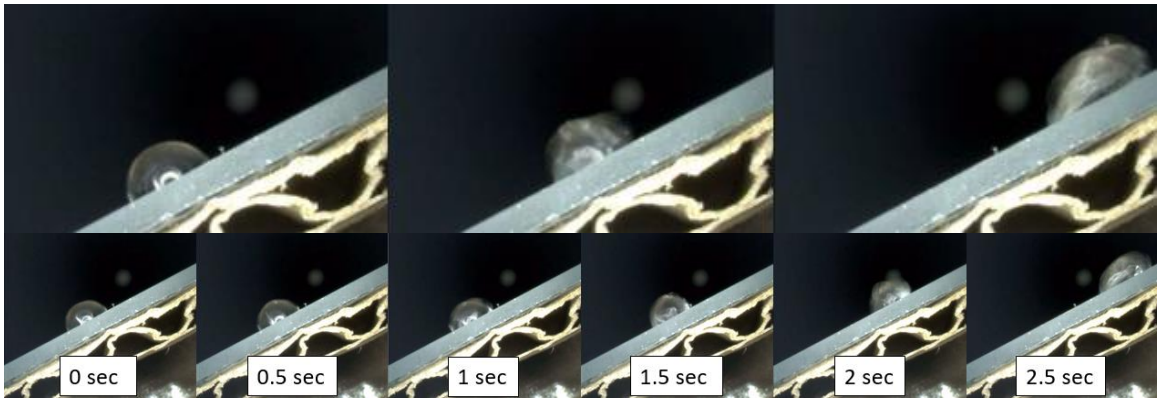

Figure B8. PMMA/PDMS